Construction and Building Materials 323 (2022) 126529

Contents lists available at ScienceDirect

Construction and Building Materials

journal homepage: www.elsevier.com/locate/conbuildmat

Review

# Thermal and fire resistance of Class F fly ash based geopolymers – A review

K.M. Klima [a], K. Schollbach [a], H.J.H. Brouwers [a], Qingliang Yu [a,b,*]

[a] Department of Built Environment, Eindhoven University of Technology, Eindhoven 5600 MB, the Netherlands
[b] School of Civil Engineering, Wuhan University, Wuhan 430072, PR China

ARTICLE INFO

*Keywords:*
Coal Combustion Fly Ash
Fire resistance
High-temperature
Geopolymers
Thermal incompatibilities
Pores interconnectivity

ABSTRACT

In recent years, the construction industry has striven to promote environmentally friendly materials. A growing body of literature has recognised fly ash-based geopolymers as a promising alternative to Portland Cement. However, a detailed and in-depth review specifically concerning high-temperature exposure and fire resistance of fly ash-based geopolymers is still missing. This review provides a comprehensive summary on the recent research progress concerning mix design, curing and their effects on thermal and fire resistance of Class F fly ash geopolymers. Due to the wide variety of characteristics, the performance of class F fly ash is recommended to be assessed in terms of its reactive phases. The influence of different alkali sources and their effects on thermal resistance are discussed, showing that potassium-based activators contribute to better performances. By applying Factsage calculations, the role of minor elements in controlling melting temperature and phase formation as well as the mechanisms behind the initial strength increase of fly ash-based geopolymers during heating are discussed. Moreover, the evolution of material properties during high-temperature exposure and the key parameter pore interconnectivity to avoid damage such as spalling is reviewed. Finally, recommendations for further investigations are provided.

## 1. Introduction

Increasing attention is being paid to the issue of fire resistance of building materials and the associated safety aspects, which are especially motivated by the numerous fires in residential buildings and public infrastructure. According to the platform FSEU (Fire Safe Europe), 2 million fires are reported in Europe each year and more importantly, 90% of them occur in buildings, partly attributed to the increased use of flammable materials. Ordinary Portland Cement (OPC) based concrete, with a worldwide production of 25 billion tons in 2018 [1], has great room-temperature performance, but its structure is weakened remarkably by the action of fire. Explosive spalling in dense concrete can be observed in the temperature range of 300 to 450 °C [2] and the loss of load-carrying capacity occurs if the temperature is higher than 400 °C due to the decomposition of portlandite [3], which causes irreversible structural changes.

Recent studies [4–6] demonstrated that geopolymers, an alternative to Portland cement, present a better fire behaviour. Research on the aspect of fire resistance originates from Davidovits' work on modern fire-retardant materials [7], as a response to the catastrophic fires involving plastics in France in 1970–1973. A major advantage of geopolymers is their strength retaining ability after high-temperature exposure. Moreover, applying geopolymers as a non-combustible construction material would have a positive impact on the environment because their $CO_2$ emissions are up to 80% lower than OPC [2]. Geopolymers, often described as anti-spalling materials [8], are produced from the reaction of an alkali source with inorganic precursors containing alumina and silica [9]. The reaction is called geopolymerization, a process by which $SiO_4$ and $AlO_4$ tetrahedrons are combined to form a three-dimensional framework structure. The reaction mechanism was described by Davidovits [10] as a polycondensation reaction:

---

* Corresponding author.
*E-mail address:* q.yu@bwk.tue.nl (Q. Yu).

https://doi.org/10.1016/j.conbuildmat.2022.126529
Received 29 October 2021; Received in revised form 12 January 2022; Accepted 18 January 2022

$$n(SiO_2, Al_2O_2) + 2nSiO_2 + 4H_2O \xrightarrow{NaOH,KOH} (Na,K)^{(+)} - \overset{|}{\underset{|}{Si}} - O - \overset{|}{\underset{|}{Al^{(-)}}} - O - \overset{|}{\underset{|}{Si}} - O-) + 4nH_2O \quad (1)$$

The inorganic 3D framework provides geopolymers with excellent thermal stability that do not generate toxic fumes during a fire, enabling their high-temperature application such as fire-resistant coatings, thermal insulation layers and wall panels [3].

In recent years, geopolymers for high-temperature applications have been widely investigated owing to the growing awareness of the importance of passive fire protection of buildings and structures, as well as the demand for cost-effective and environmentally friendly construction materials [11–18]. Research shows that the performance of fly ash-based geopolymers is strongly affected by numerous factors, such as type of alkali reagent [19], curing conditions [19], silica modulus [20], porosity [21], phase composition [22], volumetric changes [23] and thermal compatibility of the components [16]. However, many results are observed conflicting and there is still no clear consensus about mix designs as well as influential factors concerning the fire performance. Lahoti et al. [24] composed a comprehensive review on fire performance of geopolymers but it primarily focused on the degradation of geopolymers under high temperature from different scales of micro-, meso- and macro-, while the significance of influential factors mentioned above was not addressed in detail. Further, various solid precursors as well as activators were covered which make it fairly difficult to derive trends or mechanisms for certain specific materials. Understanding how to alter geopolymer mixing with single fly ash is vital but there is a lack of comprehensive study which underlines the most critical aspects of the geopolymer mix design for high-temperature application. It has been investigated that not all fly ash-based geopolymer formulations have strong thermal stability. Rickard et al. [22,25] investigated fly ash samples from different origins that provide varied high-temperature performance, implying that single system fly ash-based needs to be thoroughly investigated in terms of high-temperature resistance for designing good performing geopolymer based on locally available fly ash, both in a single or blended mixes. Therefore, a new comprehensive review with the focus on these items may help in understanding the interdependence of factors, the sensitivity of the geopolymer system to the action of high temperature and fire, and provide insight on the mix design for such applications.

In this paper, we review fly ash geopolymers related works and summarize relationships between parameters that define the initial composition, optimal preparation conditions and the expected behaviour at elevated temperatures, to obtain a guideline for fly ash geopolymers in the high-temperature application. Apart from highlighting the unique properties of fly ash geopolymers for high-temperature applications, perspectives on features that could be enhanced, and areas of research still need to be explored are also provided.

## 2. Factors affecting geopolymer properties

### 2.1. Fly ash reactivity

The focus of this review is Class F fly ash (Fig. 1) as the starting material of the geopolymers (Table 1). Class F fly ash is primarily amorphous, but also contains some crystalline phases such as quartz, mullite, iron oxides, lime and periclase [26,27].

Its reactivity in an alkaline environment is strongly related to the content of vitreous (amorphous) phase and its composition. A higher content of vitreous phase results in a faster activation and a higher degree of reactivity [29]. However, it should also be noted that the reactive phase is not entirely associated with the amorphous phase of ash. For instance, some refractory phases are not reactive but also considered as part of the fly ash amorphous phase. The crystalline components are typically non-reactive. A content of reactive silica between 40 and 50 % by mass is crucial [30], as is the amount of reactive $Al_2O_3$. However, this content can vary quite considerably, because the composition of fly ash itself is very variable and so is the ratio between amorphous and crystalline phases. This variability makes it difficult to compare results from different studies because the amount of reactive oxides is rarely determined. The chemical bulk composition (for example determined by XRF) that is often given contains no information about how the oxides are bound. This missing information is likely the reason for some conflicting results in the literature. There are existing methods which determine fly ash reactivity such as measuring the heat release and calcium hydroxide consumption in high pH environment [31] or method proposed by Pietersen [32] as the dissolution of fly ash in sodium hydroxide at different temperature 20–40 °C. It can be stated that chemical composition does not reflect reactivity. It is influenced by

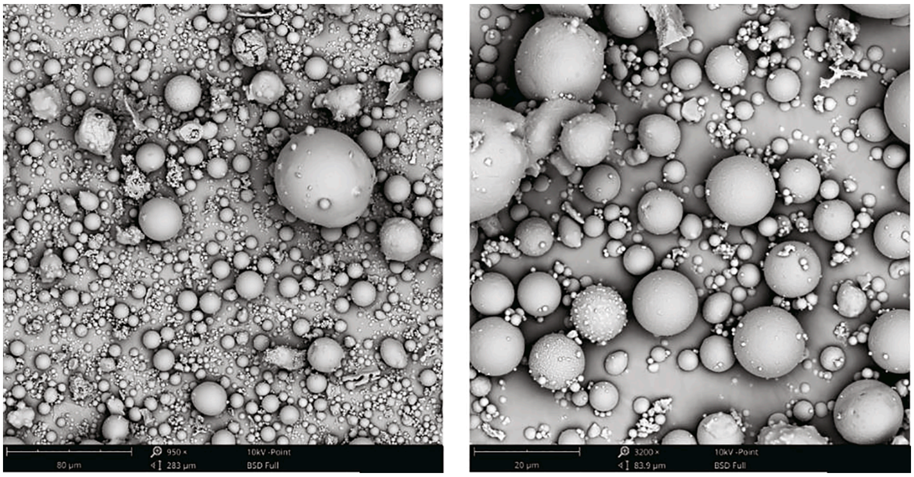

**Fig. 1.** Typical SEM of fly ash including fly ash precipitators and cenospheres.

**Table 1**
Summary of class F fly ash chemical composition ranges worldwide (approximate values based on [28]).

| % Chemical composition | | | | | | | | | | | |
|---|---|---|---|---|---|---|---|---|---|---|---|
| $SiO_2$ | $Al_2O_3$ | $Fe_2O_3$ | CaO | $K_2O$ | MgO | $SO_3$ | $TiO_2$ | $Na_2O$ | $P_2O_5$ | MnO | LOI |
| 30–70 | 15–50 | 1–30 | <10.0 | <4.0 | <4.0 | <2.00 | <3.0 | <2.0 | <2.00 | <0.5 | < 20 |

aforementioned crystalline phase contribution in the overall composition, the particle size and geometry (angularity) of the particles. Measuring the bulk chemical composition of fly ash before and after dissolution and combining it with the mass loss during dissolution would at least offer some consistent insight into the amount of reactive oxides present and the subsequent composition of reaction products. An alternative approach was proposed by Fernandez-Jimenez et al. [33], who stated that chemical analysis with hydrofluoric acid, Rietveld refinement and nuclear magnetic resonance can be combined to achieve a reasonably precise quantification of the vitreous phase materials in fly ash. One recent research [34] regarding the potential reactivity of fly for geopolymer designing showed that by combining fly ash dissolution in 10 M NaOH at 80 °C and treatment of the residue by HCl solution, the total amount of reactive Si/Al molar ratio can be reliably determined. This research underlined the main difference between Si/Al ratio obtained via XRF (1.63), vitreous based on XRD coupled with XRF (3.75) and reactive (2.65–2.98). Observations revealed a substantial reliance of the results on the time of dissolution or solution alkalinity; moreover, refractory phases may exist among the amorphous component, which, despite their amorphous structures (XRD), are not reactive. In order to compare the findings obtained and use them for further study, we recommend that any research on fly-ash geopolymers should be focused on the reactive portion of the ash.

### 2.2. Si/Al ratio

The ratio of reactive silica and alumina plays one of the most important roles in geopolymerization reactions. For example, quartz and mullite increase the ratio of Si/Al in the bulk composition, however, they do not contribute in the context of alkali activation due to their crystalline character [35], as mentioned above. The Si/Al ratio determines the thermal expansion of geopolymers; a lower thermal stability is observed with an increased Si/Al due to swelling of silica-rich secondary phases [22,36]. Further, the origin of silica and alumina plays an important role. For instance, research presented by Rickard et al. [22] showed that increasing the reactive Si/Al molar ratio from 1.15 and 1.87 to 2.0 and 3.0 respectively by adding extra silicate solution causes greater expansion and lower thermal stability of the samples and also the reduction of residual compressive strength after exposure to fire. A large portion of the excessive silicon added via solution does not react to form geopolymeric gel and the residual silicate is likely to swell at high temperature that causes strength loss after firing [22]. Provis et al. [36] explained this phenomenon in high-silica activating solution by the low amount of silicate monomers, which causes slow dissolution of fly ash particles, leading to lower amounts of Al in the geopolymeric gel and therefore lower rates of geopolymerization. The low degree of geopolymeric gel connectivity causes rapid thermal expansion. However, increasing the Si/Al ratio with more silica fume, which contains monomers, can improve compressive strength. Noteworthy, this contribution is not limited to chemical improvement; it also possesses the function of a microstructure refinement [37], by a small amount of well-distributed nanoparticles acting as a matrix compaction agent. Rodriguez et al. [38], who gave insight into the role of nanomaterial (nanosilica) in the formation of microstructure of fly ash-based geopolymer, stated that when a commercially available silicate solution was replaced with nanosilica, a denser microstructure with reduced porosity and permeability was obtained, which is directly connected to lower water demand. By enriching one mixture by 8 wt% silica fume it was possible to improve strength performance over the entire temperature range significantly (Table 2) [39]. Shaikh et al. [40] studied the impact of nanosilica (NS) and fine silica fume (SF) on the geopolymer specimens at elevated temperatures. They reported that geopolymers containing 2% and 10% of NS and SF respectively, generated mullite which is considered a desirable high-temperature phase in refractory materials [41]. As a result, lower mass loss, volumetric shrinkage and greater residual strength were observed at high temperatures [40]. Moreover, as some latest studies found, an alternative and more eco-friendly source of silica, waste glass powder, shows desirable performances. It enhanced not only the fresh state characteristics and room temperature performance but also the high-temperature related to the melting of waste glass, which improves the geopolymer gel's integrity [42,43].

**Table 2**
Compressive strength of geopolymers based on fly ash at different temperatures [39]

| Mix detail | Compressive Strength (MPa) | | | |
|---|---|---|---|---|
| | 80 °C | 600 °C | 800 °C | 1000 °C |
| Fly ash + $NaOH/Na_2SiO_3$ | 36.7 | 41.8 | 12.8 | 8.32 |
| Fly ash + 8 wt% SF + $NaOH/Na_2SiO_3$ | 67.6 | 70.1 | 34.2 | 31.34 |

It is noteworthy, that the Si/Al ratio also determines the initial temperature of the gel crystallization process, the higher the $SiO_2/Al_2O_3$ ratio, the higher the temperature of crystallization. The process of crystal formation can be harmful to the stability of material due to volumetric contraction associated with crystallisation [44]. It was also observed that a higher Si/Al ratio causes a lower water demand, higher density and lower porosity during the production of the geopolymer, which contributes to higher compressive strength and modulus of elasticity [45–47]. Krivenko and Kovalchuk [48] stated that a $SiO_2/Al_2O_3$ ratio in the geopolymer bulk composition between 2 and 4 provides the material with good mechanical performance and helps with the formation of more thermally stable crystalline phases (such as hydroxysodalite or zeolite R) in sodium-based geopolymer at high temperature, however, this can only serve as a general rule of thumb and the actual amounts of reactive alumina and silica should be considered, as mentioned in Section 2.1.

Fig. 2 shows the examples of the bulk XRF $SiO_2/Al_2O_3$ of fly ash and paste together with the strength gain/loss at high temperature. The yellow colour represents the ranges where, as the temperature rose, the strength increased in comparison to the strength measured at 20 °C, whereas the green colour represents the materials whose strength decreased after thermal exposure, which could be partially related to the percentage of added silica in the form of activator solution (see the $SiO_2/Al_2O_3$ in Fig. 2). It is observed that silica from the solution does not exhibit a clear pattern or correlation when taking into consideration the percentage enrichment of the fly ashes. As a result, determining the reactive component of the ash is of significant interest as only this information can be useful to link future research to other authors' recommendations for geopolymeric paste design.

### 2.3. Alkali reagent

The alkaline modulus $SiO_2/M_2O$ (M = K, Na) describes the ratio between the content of silica and alkalis added as a hydroxide (MOH) and silicate solutions ($M_2SiO_3$). It was previously mentioned (Section 2.2) that an excessive silicate content hinders structure formation by

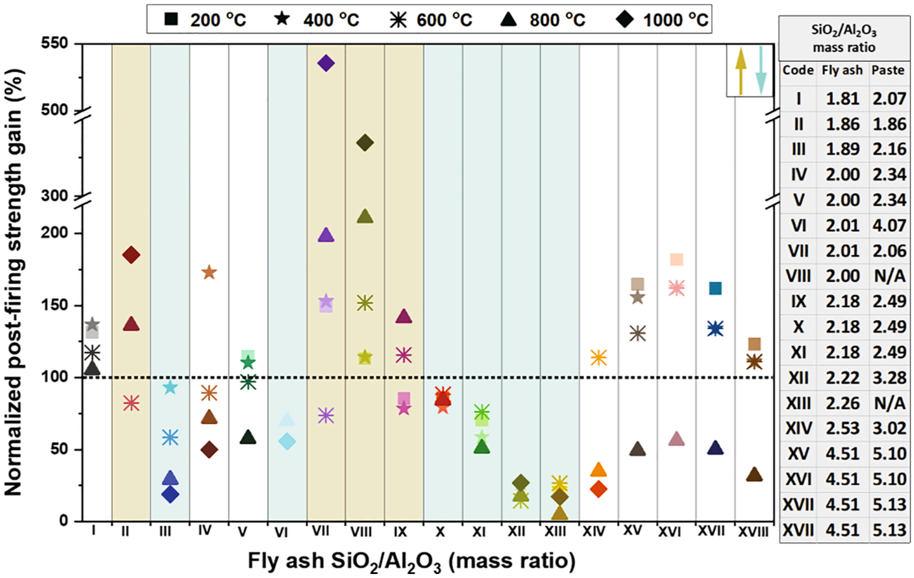

| $SiO_2/Al_2O_3$ mass ratio | | |
|---|---|---|
| Code | Fly ash | Paste |
| I | 1.81 | 2.07 |
| II | 1.86 | 1.86 |
| III | 1.89 | 2.16 |
| IV | 2.00 | 2.34 |
| V | 2.00 | 2.34 |
| VI | 2.01 | 4.07 |
| VII | 2.01 | 2.06 |
| VIII | 2.00 | N/A |
| IX | 2.18 | 2.49 |
| X | 2.18 | 2.49 |
| XI | 2.18 | 2.49 |
| XII | 2.22 | 3.28 |
| XIII | 2.26 | N/A |
| XIV | 2.53 | 3.02 |
| XV | 4.51 | 5.10 |
| XVI | 4.51 | 5.10 |
| XVII | 4.51 | 5.13 |
| XVII | 4.51 | 5.13 |

**Fig. 2.** Strength gain/loss in the temperature range 20 to 1000 °C for different $SiO_2/Al_2O_3$ weight ratio based on XRF (fly ash) and with addition of silicate from activator solution (paste). I [49]; II[50]; III [51]; IV [52]; V [40]; VI [53]; VII [23]; VIII [54]; IX-XI [55]; XII [56]; XIII [54]; XIV [39]; XV-XVIII [57].

inhibiting the geopolymerization reaction [58]. High concentrations of MOH are able to provide more hydroxyl groups to initiate geopolymerization reactions and promote gel formation [59]. Regarding potassium-based activator some discrepancies in values can be observed, for instance, the ratio $SiO_2/K_2O$ of 1.88 ($C_{KOH} = 8$ M, d = 1.33 g/cm$^3$) exhibited the highest residual strength at all range of elevated temperature treatment up to 800 °C, while Sindhunata et al. [60] stated that the best-performing specimens used the modulus ratio of 1.4. Table 3 presents these inconsistencies. It displays the silica modulus as well as the alkali cation and the major observations at elevated temperatures. The investigations that compared the thermal reactions of geopolymers with different activators (K or Na) provided a qualitative examination of the function of the alkali cation in thermal efficiency by reducing the influence of variations in fly ash composition [61,62]. Based on Table 3, it can be observed that when the potassium-based solution was used, there was a greater high-temperature performance because there was less fracture development observed and thermal shrinkage. Furthermore, the massive discrepancy between silica modulus values (from 1.0 to 1.88) and comparable findings make it difficult to determine which value is the best. The objective, however, should be to determine the reactive component of the fly ash in order to calculate overall mix ratios, such as Si/Al, Al/M (M = Na, K) and $H_2O/M_2O$. Indeed, values obtained using comparable approaches can provide a broad picture of the best ratios for high-temperature applications.

Geopolymeric gel formation is dependent on the present cations [70,71]. The initial strength of potassium-based geopolymers is lower than those activated by sodium [72] because potassium leads to the formation of more porous gels [72], however potassium-based geopolymer performance is compensated by better high-temperature behaviour. Cheng and Chiu [58] observed that the use of potassium hydroxide also results in a longer setting time, however, it also leads to a higher rate of fly ash dissolution and aluminium incorporation in the gel matrix [71]. This occurs because potassium is incorporated into the aluminosilicate framework faster than sodium due to lower charge density that is directly connected to the charge and atomic radius. Furthermore, sodium has a stronger interaction with its first hydration shell than potassium. $Na^+$ hydration sphere contains strongly bound 6 $H_2O$ molecules, whereas for $K^+$ the number is ranging from 5 to 10 [73]. Water molecules formed during the condensation of aluminosilicates will be transferred into the hydration spheres of potassium/sodium ions. From the point of energetic contributions of each hydration shell, it is more favourable for Na ions to adsorb released water molecule and K to be associated with oligomers [74].

The potassium-based geopolymers exhibit better thermomechanical properties, better thermal stability [75], lower mass loss and lower volumetric shrinkage [61] than their sodium counterparts at elevated temperatures [40]. Bakharev [76] reported that geopolymers prepared using potassium activator had higher compressive strength after fire exposure at 800 °C compared to their initial strength, while the specimens based on Na-containing activator deteriorated rapidly above 800 °C which was related to the crystallisation of Na-feldspars and a significant increase in pore size. Unlike Na-based specimens, potassium does not result in the significant crystallisation of new phases up to 1200 °C. Potassium based aluminosilicate gels have a higher temperature of decomposition than sodium ones, which explains that the $K_2O/SiO_2$ system is more suitable for fire resistance applications [35]. The decomposition at lower temperatures for a Na based system is caused by the higher diffusion coefficient of sodium at high temperature [76,77]. Pan and Sanjayan [62] concluded that the softening temperature ($T_s$, temperature at which the reversible transition in amorphous regions from a solid into a viscous state takes place) reached the highest value for K based geopolymer (800 °C) and the lowest value for mixed cation type Na/K (570 °C), while it was 610 °C for Na. The authors suggested that the mechanism determining the behaviour is similar to the one that occurs in the T-O-T structure in glass and applies to both sole and mixed alkali cations. Sodium aluminosilicate glass has a lower softening temperature than potassium glass, and mixed alkali cations (Na-K) cause a further decrease in the softening temperature [78]. This specific effect can be explained by the smaller atomic radius of sodium compared to potassium. Therefore, sodium forms stronger bonds with oxygen, resulting in a stronger inductive effect in Na-O bonds when compared to K-O bonds, and the stronger inductive effect results in lower strength at high temperatures [62]. Furthermore, Barbosa and MacKenzie [79] stated that K-based geopolymers melt only at 1400 °C and its thermal stability is related to the partial recrystallization to feldspars. In aluminosilicate systems, the presence of sodium reduces the melting temperature of the entire system by the formation of crystalline phases such as, $Na_2O{\bullet}2SiO_2$ ($T_{liquidus} = 874$ °C), $Na_2O{\bullet}SiO_2$ ($T_{liquidus} = 1089$ °C) or albite $Na_2O{\bullet}Al_2O_3{\bullet}6SiO_2$ ($T_{liquidus} = 1108$ °C). Potassium activation in low alumina systems (<10%) also reduces the melting temperature of the geopolymer due to the formation of high silica potassium silicates, such as $K_2O{\bullet}4SiO_2$ and $K_2O{\bullet}SiO_2$, with a melting temperature 770 °C

**Table 3**
Literature on molar $SiO_2/M_2O$ ratio for fly ash-based geopolymer for high temperature response tests.

| $SiO_2/M_2O$ (molar ratio)* | Ref. | Activator | T (°C) | Observations |
|---|---|---|---|---|
| **1.0** | [63] | Potassium | 700 | A slight increase in strength of GC1 is seen at 300 °C, which is attributed to sintering reaction of un-reacted fly ash particles in geopolymers. Higher splitting tensile strength of geopolymer than OPC in all temperature range from 25 to 700 °C |
| **1.14** | [6] | Sodium | 750 | Main reason of substantial degradation is dehydration above 300 °CRecommendation: changing alkali type or optimizing mix design to reduce the influence of dehydration of the degradation propagation |
| **1.15** | [64] | Sodium | 800 | No cracking observed at 800 °C. Geopolymer concrete gained strength beyond 600 °C due to the polymerization of initially unreacted material increasing |
| **1.16** | [51] | Sodium | 1000 | Faster heat transfer in geopolymeric sample than in OPC was observed, as well as better resistance to cracking of geopolymer up to 1000 °C. |
| **1.2** | [65] | Potassium-sodium | 800 | Fly ash-based geopolymer showed better performance than metakaolin-based with the same $SiO_2/M_2O$ (no cracking occurs). |
| **1.24** | [52] | Sodium | 1000 | Better performance of geopolymer than OPC both when air- and water-quenching applied. |
| **1.26** | [66] | Sodium | 800 | The further geopolymerization and sintering of the matrix cause a strength increase. This effect counteracts to another simultaneously occurring phenomenon aggregates incompatibilities |
| **1.3** | [62] | Sodium<br>Sodium/ potassium<br>potassium | 800 | The softening temperature of the geopolymer was determined only by cation used and the higher was obtained for potassium K(800 °C) > Na(610 °C) > Na/K (570 °C) |
| **1.42** | [67] | Potassium-sodium | 800 | Investigated molar ratio was 0.63 to 1.42 ($Na_2SiO_3/KOH$ mass ratio 0.5 to 2.5) in which ratio equals 1.42 (2.5) performed the best. |
| **1.43** | [61] | Sodium | 1100 | Timber coating. Specimens exhibit good fire resistance, however, K-based exhibits fewer cracks after 1100 °C than Na-based. |
| **1.43** | [68] | Sodium | 800 | Fly ash activated by Na-based solution. The investigated mass ratios $Na_2SiO_3/NaOH$ were 2.0, 2.5, and 3.0. At room temperature better mechanical performance showed sample with 2.5 ($SiO_2/Na_2O$ = 1.35), but at high temperature up to 800 °C better results were obtained for the mass ratio 3.0 ($SiO_2/Na_2O$ = 1.44) |
| **1.44** | [69] | Sodium | 800 | Blast furnace slag and Fly ash blended in weight ratio 1:1 which cause the formation of C-(N)-A-S-H Strength development until 400 °C, crystallization of the gel at 600 °C causes strength decrease and shifting porosity towards big size pores |
| **1.88** | [61] | Potassium | 1100 | Lower shrinkage and thermal conductivity of potassium-based than Na-based; |
| **1.88** | [68] | Potassium | 800 | Paste with mass ratio $K_2SiO_3/KOH$ 3.0 ($SiO_2/K_2O$ = 1.88) shows the highest residual strength. Fewer cracks, lower volumetric shrinkage and mass loss than Na-based. |

*Mass ratios $MOH/M_2SiO_3$ recalculated on the assumption that density equals: $D_{(NaOH\ 8M)} = 1.28\ g/cm^3$; $D_{(NaOH\ 10M)} = 1.33\ g/cm^3$ $D_{(NaOH\ 14M)} = 1.5\ g/cm^3$ $D_{(KOH\ 7M)} = 1.29\ g/cm^3$ $D_{(KOH\ 8M)} = 1.33\ g/cm^3$

and 976 °C respectively. However, a content of alumina above 10% results in the formation of phases such as leucite $K_2O{\bullet}Al_2O_3\ {\bullet}4SiO_2$ ($T_{liquidus} = 1693\ ^\circ C$) with a higher melting point (see Section 4). Overall, the use of K-based activator is advantageous for fly-ash based geopolymers owing to its beneficial impact on high-temperature performance, including more stable phase formation, the strength evolution and reduced mass loss and shrinkage.

### 2.4. Role of water

The properties of geopolymers are strongly determined by the amount of water in the initial solution and the content and type of residual water, such as entrapped in the small framework pores [80]. Some researchers stated that the water content has more influence on the microstructure and strength development than the chemical composition of the geopolymer gel [80–82]. Water is the medium for $OH^-$ anions that dissolve fly ash particles and hydrolyse $Al^{3+}$ and $Si^{4+}$ ions. High alkalinity is required to initiate raw material dissolution and geopolymeric gel formation that influences the reaction rate [83]. After the geopolymerization reaction, the water stays in the pores as physically bound water or gets incorporated into the geopolymer network as chemically bound water. The high $H_2O$ content causes lower strength by creating larger pores [84] and increasing pore volume which also increases the shrinkage occurring at high temperatures [25]. However, water decreases the interaction of ions by enhancing dissociation, which enhances and accelerates their transport/movement. Furthermore, an increase in the concentration of ions in the solution can be seen when ions become more mobile [85]. Thus, when $OH^-$ ions concentration in the system is high enough, more water can increase the rate of the dissolution and hydrolysis reactions through:

$$-\overset{|}{\underset{|}{Si}}-O-\overset{|}{\underset{|}{Si}}-+H_2O\overset{OH^-}{\rightarrow}2-\overset{|}{\underset{|}{Si}}-OH \tag{2}$$

$$-\overset{|}{\underset{|}{Al}}-O-\overset{|}{\underset{|}{Al}}-+H_2O\overset{OH^-}{\rightarrow}2-\overset{|}{\underset{|}{Al}}-OH \tag{3}$$

$$-\overset{|}{\underset{|}{Si}}-O-\overset{|}{\underset{|}{Al}}-+H_2O\overset{OH^-}{\rightarrow}-\overset{|}{\underset{|}{Si}}-OH+-\overset{|}{\underset{|}{Al}}-OH \tag{4}$$

This is beneficial for improving geopolymerization reaction efficiency, but at the same time, the water hinders polycondensation kinetically [86]. Barbosa and Mackenzie [87] also observed that a

**Table 4**
Differences in final Si/Al ratios of the geopolymeric gel of FA-based material cured at elevated temperatures based on the same fly ash [60]

| Curing time (h) | Curing temperature (°C) | Final Si/Al |
|---|---|---|
| 24 | 50 | 1.66 |
| 48 | 50 | 1.64 |
| 24 | 75 | 1.75 |

higher water content increases the amount of unbound sodium that can migrate to the surface over time. It undergoes atmospheric carbonation, forming $Na_2CO_3$ that undergoes a melting process after reaching 1000 °C [88], forming a glaze.

### 2.5. *Curing regime*

Different curing regimes can be applied to obtain geopolymer with good performance at room and high temperatures. Heat cured geopolymers in general are characterized by high compressive strength, low drying shrinkage and moderately low creep [51], because the higher temperatures increase the dissolution of the aluminosilicate source, thus increasing the polycondensation reaction and gel formation. Additionally, greater polycondensation shortens the setting time of the specimens.

The most typical temperature range for the initial hours (up to 24 h) of curing is 50–80 °C, followed by room temperature curing. The initial 48 h are crucial for geopolymerization reactions. Many investigations have reported that a curing temperature of 60–65 °C [89–92] and a curing duration of 24 h is the optimal. The prolonged exposure or exposure to higher temperatures is unprofitable since there was no significant improvement in compressive strength at temperatures beyond 60 °C [93]. Sindhunata et al. [60] demonstrated that temperatures over 50 ℃ promotes geopolymerization by enhancing the geopolymer's final Si / Al ratio and increasing the system reactivity (Table 4), suggesting that geopolymerization is first and foremost reliant on the curing temperature. Taking into consideration the costs associated with energy, increasing the heating duration from 24 to 40 h results in only 10% gain in strength [94], while additional heating up to 72 h results in a negligible improvement in strength, according to [89].

Curing at lower temperature (~32 °C) conditions for up to 3 days before applying high-temperature curing has been shown to be particularly effective for achieving higher strengths than the specimens cured directly at 60 °C (Tables 5) [93]. These results need further investigation, however, it seems an initially slow dissolution of aluminosilicate species during ambient temperature curing could be beneficial for further temperature-induced condensation. Nevertheless, it has to be mentioned that realistically the necessity of curing at elevated temperature limits the possibility of wide industrial application of fly ash geopolymers as fire-resistant material to the precast geopolymer concrete.

### 2.6. *The influence of minor elements on the geopolymeric microstructure*

#### 2.6.1. *Calcium*

In Class F Fly Ash (CaO < 10 wt%), calcium is present in the form of calcium silicate and aluminosilicate glasses [95]. It is believed that a small quantity of reactive calcium improves the early and late age properties of fly ash based geopolymer cured at room temperature [96–98]. Calcium plays the role of a promotor of reaction and coexisting (C-S-H) phase formation in the geopolymer matrix [99], so adding reactive calcium to class F fly ash can be beneficial. Calcium provides nucleation points for dissolved species and improves strength. As a result of the presence of calcium, small amounts of various Ca-bearing minerals are formed, such as gehlenite, anorthite, β- wollastonite [100] and hillebrandite $Ca_2SiO_3(OH)_2$. Dombrowski et al. [50] studied the influence of calcium content on fly ash based geopolymers. The fly ash initially contained 2.8 wt% CaO and the samples were modified by the addition of 8 wt% calcium hydroxide, which provided better material performance both at room and high temperature than non-modified samples. They had much higher strength after 28 days and the smallest shrinkage upon heating to 1050 °C. However, more than 8 wt% of $Ca(OH)_2$ decreased the softening temperature that plays a crucial role for high temperature behaviour [50]. In general, the addition of calcium hydroxide is more effective than the addition of free lime, which is related to the uncomplete hydration of CaO in the alkaline medium to form $Ca(OH)_2$ [101,102].

**Table 5a**
The initial composition of the geopolymer used for the calculations shown in Fig. 6 (based on Nazari et al. [52]).

| **Component** | $SiO_2$ | $Al_2O_3$ | $Fe_2O_3$ | CaO | $Na_2O$ | $K_2O$ |
|---|---|---|---|---|---|---|
| **Composition (mass%)** | 53.93 | 23.04 | 11.25 | 3.87 | 7.28 | 0.63 |

**Table 5b**
Geopolymer strength variations as low temperature curing is used prior to exposure at 60 °C curing [93].

| | Compressive strength variation (100% refers to the material directly cured at 60 °C) | |
|---|---|---|
| Low temperature curing | A (%) | B (%) |
| 1 day | 139 | 122 |
| 2 days | 146 | 130 |
| 3 days | 155 | 133 |
| 4 days | 155 | 134 |
| 5 days | 154 | 135 |

#### 2.6.2. *Iron*

Originally, iron occurs in the fly ash as hematite and magnetite, partly as an iron oxide surrounded by a sintered glass phase. However, the dominant part of iron fraction occurs in the iron-bearing glass, as cenosphere and microspheres (Fig. 3), in the form of ions $Fe^{2+}$ and $Fe^{3+}$ [103] and as particles of superparamagnetic spinel structure such as hercynite [104].

It has been stated that the iron present in raw fly ash is mainly amorphous [105,106] and the total iron content varies in a wide range from 1 to 28% (Table 1). A common phenomenon observed in fly ash-based geopolymers is colour change at high temperatures that is mainly related to the oxidation of iron from $Fe^{2+}$ to $Fe^{3+}$ [51], and in particular, a dark red colour appears due to the increased formation of hematite [105,107]. An interesting phenomenon occurs above 600 °C when the viscous sintering of aluminosilicates takes place, the high-ferrous glasses undergo melting and the amorphous iron, which can be captured in the ash spheres, can be exposed to the atmosphere and undergo oxidation reactions. Furthermore, the formation of crystalline phases occurs during the inversion of unstable maghemite ($\gamma Fe_2O_3$) to hematite ($\alpha Fe_2O_3$) [105,108], and this new crystalline product tends to form agglomerates and causes expansion at high temperatures, resulting in strength loss.

#### 2.6.3. *Magnesium*

Magnesium, like calcium, can form magnesium-containing silicate hydrates (MSH ($Mg_8Si_8O_{20}(OH)_8 \bullet (H_2O)_{12}$)) in alkali-activated materials. Its influence is generally low in fly ash-based geopolymers due to low concentrations (Table 1), but it needs to be considered when external MgO is added either directly or in the form of GGBFS. Typical GGBFS contains about 8 wt% of magnesia and it leads to the formation of hydrotalcite-like phases ($Mg_4Al_2O_7{\cdot}10H_2O$). Concerning the effect of magnesium on the thermal stability of geopolymers, the research of Yang et al. [109] about high-magnesium nickel slag incorporation can be referred. Slag obtained from the pyrometallurgical process leads to the formation of N-A-(M)-S-H gel that mitigates the structure degradation effect after high-temperature exposure. N-A-(M)-S-H gel reduces the evaporation of free and physically bound water, additionally the amount of water is significantly lower than that in N-A-S-H gel. The composition and structure modification by Mg cause an increase in the sintering temperature of gel. The obtained magnesium-silicate phases improve the thermal volumetric stability as a result of reduced thermal shrinkage. Drying shrinkage was also reduced by high-magnesium nickel slag incorporation from 0.8% to 1.6% for a solution with modulus $M_s = 1.4$. Nevertheless, as Jin et al. [110] emphasized, the

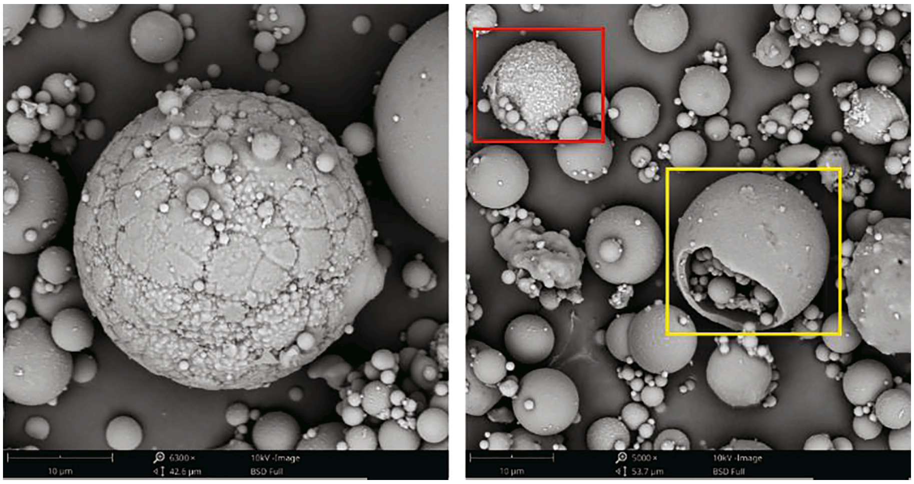

**Fig. 3.** Ferrospheres (red) present in the ash as well as ash particles trapped in the spherical structure (yellow). (For interpretation of the references to colour in this figure legend, the reader is referred to the web version of this article.)

impact on the material performance depends on the form in which magnesium occurs. However, there is still insufficient information related to the microstructure development of N-A-(M)-S-H gel behaviour at high temperature. Due to this fact, this topic requires further investigation.

### 2.7. *Zeolites*

Zeolites, a new crystalline phase present in the geopolymer structure, were recognized as the secondary reaction products during the geopolymerization process in many scientific works [111–114]. The type and content of zeolite are conditional on the raw material composition, type of alkali activator and curing conditions [115]. From the mechanical point of view, the presence of zeolites is unfavourable for the geopolymer performance, because zeolites are crystalline aluminosilicates with a variable Si/Al ratio that form a highly porous framework structure. However, it is possible to obtain the geopolymer-supported zeolite material which possesses high compressive strength (e.g. 57 MPa [116]). This effect is driven mainly by slow zeolite nucleation that enhances the development of strong crystallization contacts between zeolites and the primary gel phases [115,117,118].

Thermally stable zeolites, both in-situ and ex-situ synthesized, can enhance high-temperature performance [107] and durability. Materials that include 2.5 to 10 wt% of zeolite-like products showed good fire behaviour [48]. The thermodynamic stability of zeolites depends on the high strength of the Si-O and Al-O bonds and the stability is enhanced

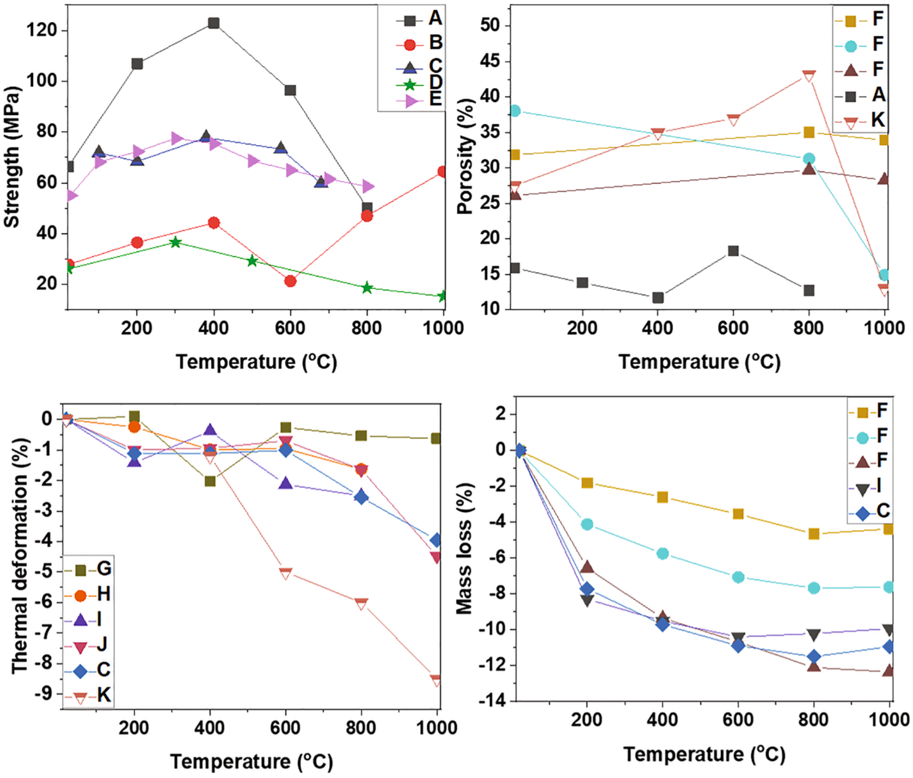

**Fig. 4.** Compressive strength, Porosity, Thermal deformation and mass loss of fly ash-based geopolymer based on literature. A [69]; B [41]; C [23]; D [126]; E [53]; F [76]; G [50]; H [127]; I [105]; J [22], K [128]

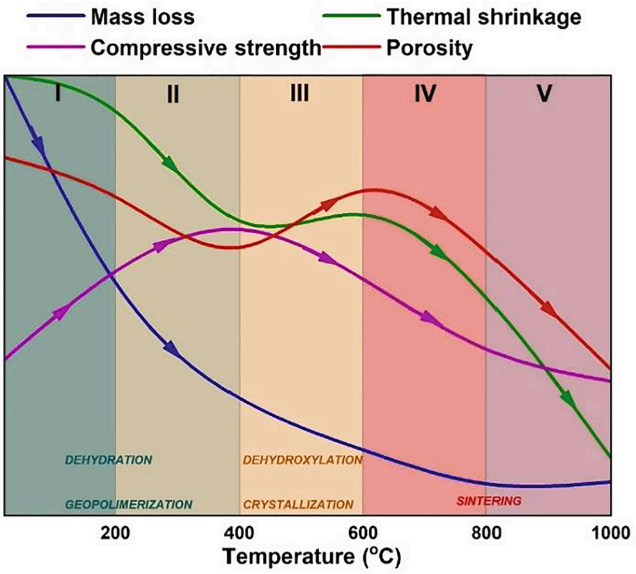

**Fig. 5.** Schematic diagram of fly ash-based geopolymer performance at high temperature. The arrows show the most significant temperature ranges for each parameter.

with a higher aluminium content [119]. The process of heating causes damages to the Si-O-Si bonds, especially in the pores and channels of zeolites. However, high temperature exposure may also be advantageous by shortening the bond length of Si-O-Si and Si-O-Al and increasing the van der Waals forces [120]. Another aspect is related to the volumetric stability of zeolites during heating. The thermal expansion coefficient of zeolites is reported to be remarkably negative, between $-3 \cdot 10^{-6}\ K^{-1}$ and $-26.1 \cdot 10^{-6}\ K^{-1}$ [121]. Moreover, zeolites have micropores and geopolymers are mainly mesoporous [122], indicating that combining them in a composite may favourably adjust the pore size distribution of the matrix [123]. Sturm et al. [124], by investigating one-part geopolymer-zeolite composite, underlined its different behaviour at high temperatures. The rapid shrinkage of geopolymers without zeolites up to 400 °C is caused mainly by the evaporation of structural water (Fig. 4), while the performance of composites containing zeolite composite obviously differs. Up to 700 °C, the shrinkage is almost linear with the maximum value ca. 2–3% in this temperature range. When compared to geopolymer without zeolites (Fig. 5), the difference in behaviour is due to the nature of water in composite, which has a more zeolitic character. Since the release of zeolitic water occurs at temperatures higher than the boiling point of water [125], less severe shrinkage is expected at temperature range of 100–200 °C than in non-modified FA-geopolymer. However, an extensive shrinkage occurring above 700 °C is caused by the structural breakdown of zeolite crystals. In the discussed case, the low- and medium-silica specimens underwent the phase change, resulting in the formation of nepheline polymorphs and carnegieite-like phase [124].

## 3. Temperature induced reactions: Mechanism and products

### 3.1. Temperature-controlled geopolymerization

The kinetics of geopolymerization are temperature controlled and can be described as inhibition kinetics [60]. After mixing fly ash with the activator, a high rate of dissolution is observed due to the high concentration of alkali and silicates. This step is followed with the nucleation and gel growth process. Elevated temperature curing (as discussed in Section 2.5) increases the dissolution of aluminosilicate species and promotes the formation of geopolymeric gel due to polycondensation reactions. Once the alkalis get incorporated into the network structure the concentration of available alkaline ions decreases; thus, the reaction is slowed down. The dissolution and polycondensation still occur but at a lower rate until equilibrium is reached. After the geopolymer has set, the reaction speed is slowed down [60].

### 3.2. High-temperature behaviour – reactions and performance

Fig. 4 shows the properties of several different fly ash based geopolymers depending on temperature. In comparison with PC, fly ash-based geopolymers become stronger with increasing temperatures up to 400 °C, which is attributed to the further geopolymerization of unreacted fly ash. At temperatures above 400 °C, decomposition is detected, and the porosity starts to rise, suggesting that these phenomena are interrelated. The crucial temperature range for thermal shrinkage is placed above 600 °C due to the sintering which also affects the porosity of the composite. An increase in the porosity at high temperature can be also observed due to thermal cracks formation. In order to make a clear view, the schematic diagram (Fig. 5) was created and divided into 5 sections where changes in the performance are visualized.

**1st step** below 200 °C: Evaporation of physically adsorbed water in the microporous structure [105]. Free water release causes the mass loss and density to decrease. Mechanical performance is improved by the temperature-induced gel formation and reduced amount of unreacted particles. The newly formed geopolymeric gel fills free space and voids.

**2nd step** 200–400 °C: high rate of contraction as a result of slow removal of chemically bound water, the shrinkage of the pores and partial pore collapse due to large capillary strain [105] and surface energy of the geopolymeric gel. Densification of the structure and continuous geopolymerization further contribute to strength development. As reported in [129], fly ash-based geopolymers can reach 158% of initial strength at 300 °C of the reference strength at room temperature due to the aforementioned continuous geopolymerization. Moreover, porosity decreases due to the filling of voids and space by geopolymeric gel.

**3rd step** 400–600 °C: low rate of shrinkage due to slow dehydroxylation, for instance, dihydroxylation of amorphous iron hydroxides and formation of hematite [105,130]

$$2FeOOH \rightarrow Fe_2O_3 + 2H_2O \tag{5}$$

The process of gel crystallization takes place, causing strength decrease as a consequence of new phases nucleation in the geopolymeric network and formation of new pores.

**4th step** 600 – 800 °C: further increase of shrinkage due to the viscous sintering of the geopolymeric matrix [22,55]. Continuous oxidation of exposed iron oxides captured in unreacted fly ash spheres and recrystallization cause weakness of the structure. Porosity decreases due to the sintering process. Formation of macropores and thermal cracking takes place.

**5th step** 800–1000 °C: continuous viscous sintering that causes more dramatic porosity decrease, thermal shrinkage and further homogenisation of the matrix.

### 3.3. Thermally-induced phase formation: feldspar and feldspathoid

Commonly occurring felspars in geopolymers are alkali feldspars, characterized by various chemical compositions or solid solutions. Orthoclase and albite are two examples of such differentiation, since their structures may include varying amounts of sodium or potassium atoms due to their (Na and K) excessive replacement of each other. The majority of feldspars found in geopolymers are triclinic and have smaller cations ($Na^{+}$, $K^{+}$, $Ca^{2+}$) in the structure. Feldspars are known to undergo various order–disorder or displacive phase transitions [131]. The temperature of crystallization depends on the alkali content in the system and the composition of solid precursors [35]. During the heating of geopolymers, non-equilibrium melt will take place and new crystalline phases are formed. As the temperature rises, so does the rate of $SiO_2$ diffusion into the reaction zone. Subsequently, thermal breakdown of non-stable crystalline structure and sintering of the matrix, which is rich in $SiO_2$ and $Al_2O_3$ particles and metal ions from raw material and activator solution, begin the primary reaction pathway. Following the creation of feldspar, the system remains stable until the temperature reaches the melting point. According to Carabba et al. [45], the crystallization of thermo-stable nepheline ($(Na,K)AlSiO_4$) and plagioclase ($(Na,Ca)Al_{1\text{-}2}Si_{3\text{-}2}O_8$) phase at 800 °C can positively influence the high-temperature performance by reducing the thermal conductivity of the geopolymer paste; plagioclase is a poor heat conductor [132] and the nepheline reduces the thermal diffusion of geopolymer due to the increased volume fraction [45,133]. Furthermore, Alehyen et al. [134] stated that the presence of sodium-contained feldspar (albite) can help to maintain mechanical performance during high-temperature exposure and its formation in geopolymer matrix at 1000 °C was confirmed by another research [17]. Therefore, fully understanding the thermal properties of feldspars allows for further geopolymer's modification, such as adding different feldspars to a fly ash-based geopolymer, which can be beneficial for high-temperature application and durability, as shown by Kumar and Mayengbam [135].

The production of feldspathoid (leucite) in potassium-rich geopolymer is most likely induced by the lack of $SiO_2$ in the reaction zone and by $K_2O$ site saturation. For fly ash-based geopolymeric samples, the temperatures between 550 and 650 °C are important when the change of the porosity and pore size distribution occurs. These changes are mostly related to the glass transition temperature and viscoelastic behaviour of the solids [22,62,126], meanwhile crystallization of the nepheline and plagioclase phases from amorphous gel takes place [45]. Thakur [136] and Duxson [82] observed that crystallization occurring during the heating improved the compressive strength of specimens. The suggested phase formation mechanism is suitable for both potassium and sodium activated geopolymers. However, the temperature of the phase formations would be conditional on the used activator. Regarding the phase changes, it can be summarized:

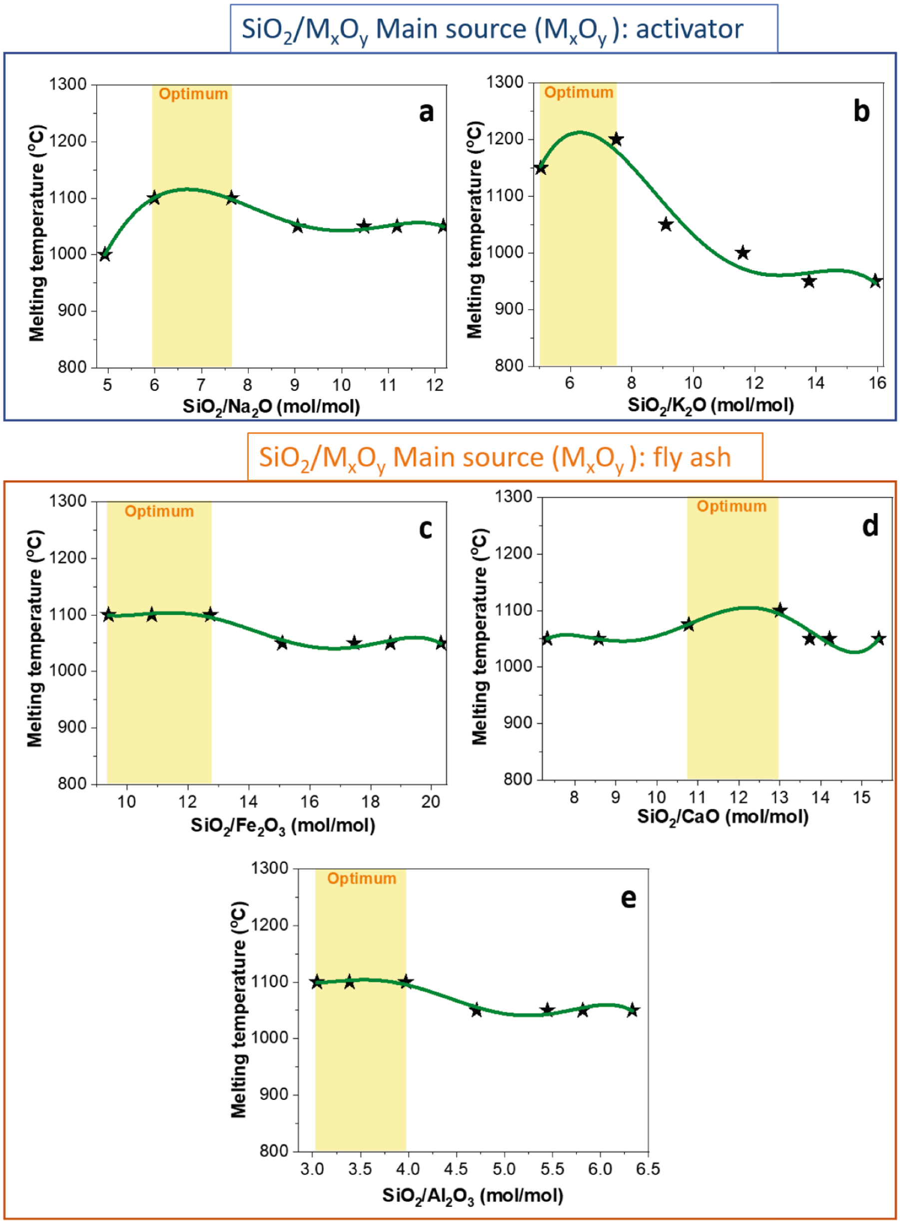

**Fig. 6.** The effect of molar ratio on the initial melting point of the geopolymer using FactSage thermodynamic calculations. Note: Fig. 6b based on K activator, while **6a, c, d, e** are based on Na. (Composition shown in **Table 5**).

- 600–900 °C: low silica crystals feldspathoid group (nepheline (Na-system), kaliophilite (K-system)).
- 900–1200 °C: high-silica feldspars (labradorite (Na-system), leucite (K-system)).
- Above 1300 °C: redistribution of phases based on thermodynamic stability (melting).

### 3.4. *The influences of the geopolymer mix composition on onset melting temperature*

The main component in a geopolymer matrix is the geopolymeric gel together with the unreacted raw materials. The chemical composition of gels determines the melting temperature and therefore the thermal stability of the entire geopolymer at high temperatures. Thermodynamic calculations can be used to predict this behaviour, as the reactions during heating are complex and hard to determine in situ, because most of the phases involved are amorphous. Fig. 6 shows some calculations that were carried out with FactSage to illustrate the effect of the chemical composition on the melting temperature of a geopolymer. Tables 5 shows the starting composition that was used, which is based on Nazari et al. [52]. Only two oxides were varied at a time to achieve the elemental ratios shown, while the rest were kept fixed. The ratios were chosen to represent typical values found in geopolymers [54,76,111,137,138].

The melting temperature is defined as the temperature when the last melt disappeared during cooling from a starting temperature of 1500 ℃. It should be noted that volatiles were excluded from the calculation and that FactSage thermodynamic calculations [139] are based on phase equilibria. Geopolymer systems are not in equilibrium unless they are heated very slowly, which is usually not the case. The results in Fig. 6 are therefore only meant as a qualitative overview of the influence of oxide composition on the melting temperature of geopolymers.

When the influence of sodium and potassium activation is compared, it can be observed that potassium generally results in higher melting temperatures than sodium activation, which is consistent with other experimental results [62]. Further, in both cases increased activator dosage results in lower melting temperatures. This is not surprising, because the geopolymer gel forms a glass during heating and $Na_2O$ and $K_2O$ are known network modifiers that lower the melting temperature [140]. In general, the type and amount of activator has the largest influence on the resulting melting temperature. Changes in the $SiO_2/CaO$, $SiO_2/Al_2O_3$ and $SiO_2/Fe_2O_3$ ratios have much more limited effects.

## 4. Microstructure evolution under elevated temperature

### 4.1. *Pore structure*

The pore structure is formed during the gel formation and the heating leads to the evaporation of the water accumulated in the pores and channels (Fig. 5). The pores connectivity enables the water transport through the matrix and thus reduces spalling at high temperatures. In the other case, the high stress in the pore walls during the transfer of unbound water causes the pore collapse and development of shrinkage cracking. During the gel formation, the large pores are filled and the Si–O–Al-network (chains and branches) is formed, this porous structure has a mainly mesoporous character [60]. Wide pores that are not filled are macropores that can occur in the fly-ash-based geopolymers which are cured at medium temperature (~50 °C), while pores greater than 200 nm are found in geopolymers produced in a low-reactive system, for example, when geopolymer is cured at low (ambient) temperature. Fly ash-based geopolymers are characterized by a higher content of small-size pores when compared to metakaolin-based material (Table 6) [65].

**Table 6**
Comparison of the pore size percentage of the geopolymers based on metakaolin and fly ash at room temperature after 1 year [65].

| IUPAC classification | Metakaolin geopolymer (%) | Fly ash geopolymer (%) |
|---|---|---|
| Micropores (<1.25 nm) | 0.5 | 24.6 |
| Mesopores (1.25 – 25 nm) | 94.2 | 71.3 |
| Macropores (25 – 5000 nm) | 1.8 | 2.6 |
| Air voids/cracks (5000 – 500000 nm) | 3.5 | 1.5 |

**Table 7**
Fly ash-based geopolymer under high temperature [19]

| | Total intrusion volume (ml/g) | | |
|---|---|---|---|
| T (°C) | Na-based | Na/K-based | K-based |
| 25 | 0.232 | 0.231 | 0.212 |
| 500 | 0.253 | 0.252 | 0.212 |
| 900 | 0.166 | 0.208 | 0.223 |

During the formation of geopolymeric gel, the voids and space are filled, resulting in the generation of mesopores and the decrease of macropores. Pores larger than 200 nm are obtained when the curing temperature is too low (e.g. below 30 °C) or the activation is based only on hydroxide solution [60]. Sindhunata et al. [60] derived the relation between $SiO_2/M_2O$ ratio of alkali solution and porosity. Increasing the $SiO_2/M_2O$ ratio from 0.79 to 2.0 causes an increase in mesopore volume and surface area. More mesopores demonstrate a higher rate of geopolymer gel formation, for potassium activated fly ash, 1.4 is considered as the optimal ratio. Samples with a ratio lower than 1.4 contain larger particles of aluminosilicate gel, thus a higher porosity of the material is observed [60]. The pore volume (Table 7) and pore size distribution of geopolymers based on fly ash also differ based on the alkali cation. K-based material shows a wider range of pore diameter than the sodium counterpart due to more significant structural disorder which results in the presence of larger silicate and aluminosilicate species in the matrix [141].

Sodium based and mixed alkali system revealed a total pore volume and pore size rise related to the development of cracks, while K-based remained stable. The cumulative number of pores found in samples was marginally decreased in the order of Na > NaK > Na after exposure to 900 °C while cumulative pores in K-based were slightly increased. Regarding pore size, it was observed that at 900 °C both K- and Na-base geopolymer show pore size increase, mainly due to the sintering process, however, the total pore volume is significantly reduced for sodium-based systems while it barely changes in the K-based system those differences can be related to the sintering phase densification.

### 4.2. *Fire induced spalling*

The gel microstructure and pore morphology, as indicated in the previous subsection, affect the potential of high-temperature spalling [142,143], which is the primary cause of thermally-induced material deterioration. Ozawa and Shaikh [11] confirmed the enhanced spalling resistance of the fly ash-based geopolymer compared to both the cement-based mix and the slag-enriched blends. When exposed to high temperatures, all of the specimens degraded severely, however the FA-based system only showed micro-cracking. Furthermore, as compared to other mixtures, FA-based geopolymer mortar did not show abrupt increase and following rapid fall in vapour pressure. The blends and single FA systems had maximum fracture depths of 40 mm and 0 mm, respectively. According to previous research, a blended system based on fly ash enriched with slag has a lower proportion of large and medium capillary pores in the matrix [144], which directly affect the likelihood of spalling, as this phenomenon occurs during excessive heating/contact with fire when the water vapour moves towards the cooler part of the material. Because of the lower temperature, the water vapour condenses to create a layer, which limits further transport of water vapour, resulting in high vapour pressure. Thus, the increased water content trapped in the structure and the more packed structure indicated above are the main reasons why the blended system, despite the geopolymer structure, did not demonstrate superior spalling resistance.

Other investigations have corroborated the good stability of the FA-geopolymer structures [145], including Sarker and McBeath [146] and Colangelo et al. [147], who also validated both the structure's stability in heating cycles and the lack of spalling after exposure to a temperature around 1000 °C. As noted in the preceding section, porosity, and more specifically combined open porosity, plays a critical role on the enhanced spalling resistance of fly ash containing composite [148] compared to OPC-based. However, there is still a lack of thorough understanding of the subject, which requires further assessment.

### 4.3. The evolution of physical and structural properties in terms of density

The quantitative analysis of the bulk density gives information regarding the thermally induced changes that take place during firing. The bulk density change during firing is associated with the mass loss and volumetric shrinkage of the sample as well as the porosity changes. The sample density variation is caused mainly by two effects [149]:

- Density reduction due to mass reduction (loss of free and chemically bound water and loosely packed matrix) (up to 400 °C).
- Density increase attributed to the sintering of aluminosilicates in the temperature range of 600 – 850 °C.

These density changes are also associated with the changes in strength during and after contact with fire. However, when looking at the materials not in the direction of in bulk density fluctuation, but the density of the skeleton, it is important to notice the positive influence of matrix densification at the temperature of 500 °C as a consequence of the continuity of geopolymerization reactions, which induces the improvement in structural strength. Then the geopolymer skeleton densification occurs as a result of the melting of the matrix, the melting process induces crack healing, which contributes to a better strength after exposure above 500 °C. Such variations can be more or less visible depending on the activator used, as shown by Lahoti et al. [19] that densification is noticeable according to the $K < NaK < Na$. That implies that K-geopolymer is more prone to densification than sodium counterpart. Noteworthy, as shown by Vickers et al. [23], the density of fly ash based geopolymer changes with the addition of wollastonite and α-alumina fillers [23]. The addition of the fillers, characterized by high density, increases the density of the geopolymers.

#### 4.3.1. Mass loss

The mass loss of a geopolymer during heating causes the deterioration of the material, mitigation of the mass loss is therefore desirable. It occurs as a result of significant loss of free and pore water up to 250 °C [51,150], and further up to 800 °C due to the polymerization reaction of free hydroxyl groups T-OH (T = Si, Al) (Eq. (9)) [71]. Above 300 °C the decomposition of metal-OH groups compounds also takes place [151]:

- Acids: M–O–H+ (Si(IV), Ti(IV), Fe(III))
- Basics: M + HO–hydroxide (Na, Ca (II), K, Mg (II))
- Neutral: M–OH hydroxyl (Al (III), Mn (III))

The most crucial range regarding mass loss is between 20 and 300 °C, which is responsible for about 80% of total weight loss that is attributed to the loss of adsorbed water and water removed from geopolymeric gel [105,130]. Further mass loss is related to the water release during gel condensation and its polymerization [4,129]. Above 700 °C, condensation of silanol and aluminol groups on the geopolymeric gel and water removal occur.

$$\equiv T-OH+HO-T\equiv \rightarrow \equiv T-O-T\equiv +H_2O \tag{9}$$

Kovárik et al. [152] showed that the temperature range from 800 to 1000 °C is characterized by a stable mass [153] and the decomposition of geopolymers at a temperature of about 1000 °C is caused mainly by the melting process. Generally the mass loss for a fly ash geopolymer is lower than that for GGBFS [154]. Better results are also obtained if the activator is based on potassium rather than that sodium [39]. Potassium-based geopolymer contains mainly pore water and water present as a hydration shell of present in the structure cations which is released up to 200 °C [80].

#### 4.3.2. Thermal shrinkage

Thermal shrinkage is a phenomenon in which a sample is subject to the size/volume changes due to temperature exposure. Also, local temperature differences in the sample or differences between the temperature and the surroundings can cause cracks formation. The thermal shrinkage is determined by several parameters, for instance, raw material, type of activator and curing regime [25,40,51]. The crucial temperature range for thermal shrinkage is between 200 and 350 °C, in particular, due to the water evaporation and pores collapsing and above 600 °C when the sintering process occurs. Those volumetric instabilities cause cracks formation and shape deformations, the presence of which precludes the use of the material for fire-resistance purposes. The first step in minimizing the occurrence of this negative phenomenon is to adjust the composition of the paste, both in terms of the chemical/mineralogical composition ensuring high-temperature stability (high melting temperature) as well as the pore structure allowing the non-explosive water evaporation during heating. From the chemical point of view, magnesium silicate and bound calcium have the ability to reduce thermal contraction. Furthermore, the common treatment to minimize thermal contraction is the use of thermally stable fillers and the minimization of water contained in the geopolymeric structure. The selection of fillers and aggregates is driven by their properties such as moisture sorption, specific surface area, melting points and compatibility to the matrix thermal expansion coefficient. The proper selection of the filler can substantially reduce thermal shrinkage by up to 60% at

**Table 8**
Influences of aggregates on high-temperature performance of geopolymer-based concrete.

| Ref. | Aggregates/Fillers | Exposure Temp (°C) | Observations |
|---|---|---|---|
| [63] | Graded gravel and sand | 700 | The bond degradation above 300 °C. |
| [6] | Quartz and expanded clay | 750 | Quartz: higher strength, poor thermal properties - high thermal expansion, greater strength loss.<br>Expanded clay: low strength value at room temperature and low thermal expansion |
| [64] | Rubber tire fibres. Crushed basalt and river sand | 800 | The hairline cracks in rubberized geopolymer concrete above 600 °C. |
| [66] | Sand | 800 | Strength gain or loss determined by sintering, geopolymerization and thermal incompatibility between matrix and aggregates. |
| [67] | Crushed basalt and slag aggregate | 800 | Used basalt or slag aggregates cause the reduction of strength after temperature exposure. |
| [51] | Crushed granite | 1000 | At 1000 °C the tension generated by the differential expansion between the geopolymer matrix and the aggregates. |
| [52] | Sand and gravel | 1000 | Better performance of geopolymer than OPC both when air- and water-quenching applied. Cracking appearing in both OPC and geopolymer concrete at 1000 °C |
| [61] | Carbon and basalt fibres | 1100 | Timber coating. Additives of carbon or basalt fibres decreased the char depth. Carbon fibres shows better performance than basalt. |

1000 °C as reported by Vickers et al. [23]. The phenomenon of shrinkage reduction by fillers application can be explained by the hydrogen bond formation on the filler's surface that influences the content of water release [23].

## 5. Fillers, fibres and aggregates

Fillers and aggregates are very important for fire performance. Their counterparts suitable for high-temperature applications should have high thermal stability themselves, higher or similar to the geopolymer paste. They may also undergo a thermal reaction that can positively influence the matrix by improving strength through sintering or bonding with the matrix. Furthermore, it is extremely important that their thermal expansion/shrinkage is similar to that of the geopolymer itself. Several examples of the use of various aggregates, along with the thermal reaction of concrete, are presented below (Table 8**)**. It provides a picture of the negative and positive effects of aggregates and fillers at different exposure temperatures.

### *5.1. Fillers (maximum grain size of 125 μm) and fibres*

By applying fillers and fibres it is possible to reduce internal tension and the propagation of microcracks, which helps to improve the strength of the material. What is more, the incorporation of fibres can stabilize the thermal expansion and promote the retention of mechanical strength at temperatures up to 1000 °C [44]. The key role of fillers and fibres plays to control the thermal expansion of geopolymer are their thermal expansion coefficient in the target temperature range [23]. Moreover, fillers lead to a shrinkage reduction and strength improvement during the curing of the geopolymer. The length of the fiber determines its reinforcement capacity [155]. For instance, Rahman and Radford [155] used nanofillers such as silicon carbon whiskers and stated that at high temperature, longer nanofillers perform better than their shorter counterparts. The authors [155] suggested that the length of a nanofiller should be higher than at least twice the sum of particle size and interparticle distance in a geopolymer network. Above 350 °C, the toughness of the geopolymer linearly depends on the length of nanofillers. It was suggested that the sample failure is mainly caused by the tensile failure of nanofibres over the interfacial separation. Rahman and Radford [155] stated that the weak interface between filler and matrix is better for crack energy dissipation. Bernal et al. [44] proposed 15 vol% of filler particles (milled refractory bricks average particle size 203.2 μm) and 1.0 vol% fibres (alumina-silica-zirconia fibre 3.5 μm, length 20–35 mm) to maintain the compressive strength at high temperature and reduce volumetric contraction. Furthermore, studies on the addition of 2% of nano- $TiO_2$ [156] have shown that the additive has favourable benefits, such as improving strength at room temperature by increasing the solubility of $Si^{4+}$ and $Al^{3+}$ from fly ash, as well as minimizing thermal degradation of geopolymer. Incorporation of 15 vol% small size bricks particles, characterized by low thermal expansion, provides better performance both at room and high temperature than unreinforced or with 10 vol% incorporation. A higher content of filler particles shows a higher degree of macrocracking in the geopolymer matrix after high-temperature exposure that influences the residual strength of the samples. Furthermore, it was observed that 10 vol% of milled refractory bricks does not influence the ductility but increases its mechanical performance at high temperature by creating the hurdle on the cracks propagation path [44]. Carbon and basalt fibres have also shown promising results [61]. However, carbon fibres perform better because of their greater thermal conductivity and higher heat diffusion which can facilitate heat transport. It is noteworthy that the application of wollastonite fibre ($TEC_{25\text{-}800^{\circ}C} = 6.5 \times 10^{-6}\ K^{-1}$) in fly ash based geopolymer (10 vol%) leads to both compressive and flexural strength improvement in comparison to the control sample. Wollastonite reacts with the geopolymer matrix, promoting a dense microstructure and through that provides high compressive and flexural strength. The filler's surface reactions are possible due to surface defects and high surface energy. The filler's surface reaction influences also the performance after firing, as a result of which at 1000 °C the sample gains strength by 156% compared to the sample at room temperature. This significant change was accompanied with relatively low thermal shrinkage and mass loss [23].

### *5.2. Aggregates (minimum grain size of 125 μm)*

The properties of geopolymers (e.g. residual compressive strength) are strongly related to the nature of the applied aggregates. The aggregates should be stable and non-reactive or alternatively, show positive reactivity at high temperatures. They need to possess a low volumetric expansion compatible with the paste and high strength at high temperature. Rickard et al. [6] showed that quartz aggregates are not suitable for high-temperature application due to their rapid high thermal expansion at 573 °C, when the α-β phase transition takes place. Sarker [146] observed a decrease in strength of up to 65% attributed to the incompatibility between the thermal expansion between river sand aggregates (1.2–2.5%) and the geopolymer paste (1.6%).

Particles such as ceramic spheres have good thermal stability and can make geopolymeric material more stable during the fire exposure. However, aggregates with a high angularity such as milled refractory brick are preferred, because they show a strong interaction between matrix and aggregate that results in good load transfer of the material [44].

Temperature-induced strength decrease in a geopolymer concrete in the temperature range between 400 °C and 600 °C is generally caused by incompatibility of aggregates and matrix, dehydroxylation reaction and dehydration. It can be concluded that the size, geometry and thermo-physical properties of aggregates greatly affect the concrete behaviour during the fire.

## 6. Future directions

Apart from the above discussed topics, a number of new directions that have been developed in recent years require special consideration in the future.

### *6.1. Coupling effects of environmental and thermal loadings on geopolymer durability*

Continuation of the in-depth research on the effect of weathering on the properties of fire-resistant geopolymers on fly ash bases is highly recommended. This research allows for guiding the potential production and application of the composite (tunnel protection, building interior protection). For instance, there is no reliable information on the long-term properties of these materials, whether and how fly ash-based geopolymers lose their thermal and fire-resistant properties. Thus, more research should focus on the analysis of parameters of fire-resistant materials after longer periods than the standard 28 days. Besides, most of the current research suggests that FA-based geopolymers have favourable characteristics, although most studies focus on sole heat exposure. Thus, the authors believe that further research into whether material rehabilitation or replacement is necessary after long composite exposure cycles is also a worthwhile consideration. Furthermore, external factors, such as moisture content [148], atmospheric precipitation, or chemical attack cycles, such as hydrocarbon fluids [157] and their impact on high-temperature properties is of great need.

### *6.2. Blended systems*

As mentioned in introduction, this review paper focuses on pure fly ash-based systems, however, blended systems can offer an improvement of solely FA-based geopolymer pastes, especially considering its slow reaction rate under ambient conditions. However, when it comes to mixing, the hybrid gel composition should be taken into account, as it may be helpful for room temperature performance but maybe hostile to a pure FA-based mix. For instance, the thermal transition of the C-A-S-H and N-A-S-H gel mixture based on Coal Combustion Fly Ash should be thoroughly elaborated, and the resultant phases may be used to analyse their influence on geopolymer behaviour at high temperatures. Furthermore, the microstructure evolution of a geopolymeric gel supported by magnesium (N-A-M–S–H) has not been systematically presented to assess its impact on the high-temperature performance of geopolymers including Mg-rich precursor. Recent studies have shown that it is feasible to increase FA-based geopolymer high-temperature characteristics by blending it with other materials, such as dolomite dolomite [158] or metakaolin [59], in order to achieve this goal. Thus, further investigation and use of other industrial wastes in blends, such as various slags (e.g. zinc or ferronickel slag), which can either improve material parameters at room temperature without compromising temperature resistance or enhance high-temperature resistance by introducing new crystalline and amorphous phases, would be recommended.

### 6.3. *Geopolymer foam concrete (GFC)*

GFC is made by introducing large voids into geopolymer slurry by various foaming methods [15,159,160]. By decreasing thermo-mechanical stresses at high-temperature, they exhibit improved performance. Based on our knowledge and observations, this trend has emerged more prominently in the field of fire protection of geopolymers based on Class F fly ash in recent years [161]. Owing to the very porous structure of GFC, they possess low thermal conductivity. Thus, thanks to the decreased heat flow, these composites can perform protective functions as passive fire protection/thermal barriers. Additional studies, such as on rheology and its alterations, will be required for the production of porous boards/panels or spray-applied materials. However, this topic suffers from lack of sufficient study of durability, lifetime assessment and research in relation to an upscaling process and application, as is the case for standard geopolymers. Additionally, more attention should be paid into the insulation capacity measurement via standard heating regimes, such as ISO 834, as well as shrinkage behaviour during thermal exposure.

### 6.4. *Alternative applications*

Fly ash geopolymers have good thermal characteristics, as demonstrated in this study. Besides serving as passive fire protection, interesting use of the FA-based composite's features is creating a low-cost alternative to conventional molten salt 2-tank storage for high temperatures thermal energy storage [162]. This research presents the indirect use of superior thermal characteristics such as geopolymer's excellent specific heat capacity. Another alternative application is utilizing FA-based geopolymer as a superior alternative binder for PC concrete in the new building of rigid airbase paves [157] that is related to good resistance to heat and chemical attack. Such considerations on the usage of fly ash-based geopolymer properties at elevated temperatures, according to the authors, may expand the field of application.

## 7. Concluding remarks

This review summarizes the comprehensive studies conducted during the last decades regarding Class F fly ash geopolymers for high-temperature and fire- applications. The important factors such as phase-mineral composition, melting point, volume stability and zeolites dosage are summarized that would contribute toward synergy of thermal stability and strength development. The following conclusions are drawn from this study:

- The phase composition of fly ash differs from other commonly used solid precursors, such as GGBFS or metakaolin by high crystalline content. The research on the suitability of FA-based geopolymer for high-temperature application should be based on the reactive phases of fly ash. The phase composition of activated fly ash reveals that crystalline phases remain the same as in the raw material. Due to that, designing a clear guideline based on conducted research is difficult to validate due to discrepancies in the characteristics of fly ash and its reactivity. This analysis would influence the material on design level by enriching the mixture with silica, alumina, calcium source and calculating silica modulus and the sufficient alkali content. Specifying the suitable $SiO_2/M_2O$ ratio due to inconsistency in presented results is not currently possible.
- One factor affecting material stability is the initial melting temperature. Thermodynamic calculations of the sensitivity of the fly ash-based system reveal that the temperature of melting is mostly affected by the type and amount of alkali in the system. The influence of the variations of $SiO_2/MO$ ratios (where, M = Al, Fe, Ca) on the initial melting temperature can be negligible. Nevertheless, the form (vitreous, crystalline) in which Si, Al and minor elements (Ca, Fe and Mg) occurs has a fundamental role in fly-ash reactivity and thermally induced phase transformations.
- Proposed diagram showing the behaviour of Fly ash-geopolymer during temperature exposure differs from geopolymers based on other precursors and the observations can be made on the basis of this. The phenomenon of the strength increase of fly ash-based geopolymers at high temperature in the first stage of heating (up to 400 °C) is attributed to thermally stimulated dissolution of the particles, such as fly ash cenospheres and, temperature-induced geopolymerization reaction. Moreover, it is important to stabilize contraction and thermal cracks formation in the ranges 200–400 °C and 600–800 °C to provide high-temperature-stable fly ash geopolymer. Volumetric and strength stability at high temperatures can be improved by applying aggregates, and fibres, such as wollastonite or carbon fibres. In that case, the thermal stability and thermal expansion coefficient should be comparable with the matrix.
- Despite the range in which the zeolites improve the thermal properties of the composite (2.5 to 10 wt%), it is believed that the influence of zeolite on fire resistivity of fly ash geopolymer cannot be unanimously evaluated due to the properties that vary among the zeolite group. The type of zeolite, the temperature of nucleation and structure breakdown determine its role as a high-temperature backbone of the composite.
- Further study is needed in several areas, including the durability and long-term performance of fly ash-based composites, as well as systematic research on the fire resistance of fly ash-based mixes with other wastes and by-products. It is also worth mentioning that changing the microstructure of foamed composites and exploiting their promising thermal response in a number of applications other than passive fire prevention may be accomplished.

## Declaration of Competing Interest

The authors declare that they have no known competing financial interests or personal relationships that could have appeared to influence the work reported in this paper.

## Acknowledgement

This research was carried out under project number S17013a in the framework of the Partnership Program of the Materials innovation institute M2i (www.m2i.nl) and the Technology Foundation TTW (www.stw.nl), which is part of the Netherlands Organization for Scientific Research (www.nwo.nl) (Project No. 16347).

## References

[1] https://www.grandviewresearch.com/, Fire protection Materials Market for Construction Inudstry Analysis Report, (n.d.). https://www.grandviewresearch.com/industry-analysis/fire-protection-materials-market/methodology.

[2] K.D. Hertz, Limits of spalling of fire-exposed concrete, Fire Saf. J. 38 (2) (2003) 103–116, https://doi.org/10.1016/S0379-7112(02)00051-6.

[3] L. Alarcon-Ruiz, G. Platret, E. Massieu, A. Ehrlacher, The use of thermal analysis in assessing the effect of temperature on a cement paste, Cem. Concr. Res. 35 (3) (2005) 609–613, https://doi.org/10.1016/j.cemconres.2004.06.015.

[4] P. Duxson, G.C. Lukey, J.S.J. van Deventer, Thermal evolution of metakaolin geopolymers: part 1 - physical evolution, J. Non. Cryst. Solids. 352 (52-54) (2006) 5541–5555, https://doi.org/10.1016/j.jnoncrysol.2006.09.019.

[5] W.D.A. Rickard, C.D. Borstel, A. Van Riessen, The effect of pre-treatment on the thermal performance of fly ash geopolymers, Thermochim. Acta. 573 (2013) 130–137, https://doi.org/10.1016/j.tca.2013.09.030.

[6] W.D.A. Rickard, G.J.G. Gluth, K. Pistol, In-situ thermo-mechanical testing of fly ash geopolymer concretes made with quartz and expanded clay aggregates, Cem. Concr. Res. 80 (2016) 33–43, https://doi.org/10.1016/j.cemconres.2015.11.006.

[7] P.J. Davidovits, 30 Years of Successes and Failures in Geopolymer Applications. Market Trends and Potential Breakthroughs, Clim. Chang. 2013 - Phys. Sci. Basis. (2002) 1–30. doi:10.1017/CBO9781107415324.004.

[8] Z. Tang, W. Li, Y. Hu, J.L. Zhou, V.W.Y. Tam, Review on designs and properties of multifunctional alkali-activated materials (AAMs), Constr. Build. Mater. 200 (2019) 474–489, https://doi.org/10.1016/j.conbuildmat.2018.12.157.

[9] J. Davidovits, Geopolymer cement, A Rev. Geopolymer Institute, Tech. Pap. 21 (2013) 1–11.

[10] J. Davidovits, Properties of Geopolymer Cements, First Int. Conf. Alkaline Cem. Concr. (1994).

[11] M. Ozawa, F.U.A. Shaikh, A study on spalling behaviour of geopolymer mortars using ring restraint test, Constr. Build. Mater. 279 (2021) 122494, https://doi.org/10.1016/j.conbuildmat.2021.122494.

[12] V.S. Le, P. Louda, Research of curing time and temperature-dependent strengths and fire resistance of geopolymer foam coated on an aluminum plate, Coatings. 11 (2021) 87.

[13] J.C. Kuri, S. Majhi, P.K. Sarker, A. Mukherjee, Microstructural and non-destructive investigation of the effect of high temperature exposure on ground ferronickel slag blended fly ash geopolymer mortars, J. Build. Eng. 43 (2021) 103099, https://doi.org/10.1016/j.jobe.2021.103099.

[14] I. Hager, M. Sitarz, K. Mróz, Fly-ash based geopolymer mortar for high-temperature application–Effect of slag addition, J. Clean. Prod. 316 (2021) 128168, https://doi.org/10.1016/j.jclepro.2021.128168.

[15] K. Traven, M. Češnovar, S.D. Škapin, V. Ducman, High temperature resistant fly-ash and metakaolin-based alkali-activated foams, Ceram. Int. 47 (17) (2021) 25105–25120.

[16] M. Sivasakthi, R. Jeyalakshmi, N.P. Rajamane, Fly ash geopolymer mortar: Impact of the substitution of river sand by copper slag as a fine aggregate on its thermal resistance properties, J. Clean. Prod. 279 (2021), 123766.

[17] O.H. Li, L. Yun-Ming, H. Cheng-Yong, R. Bayuaji, M.M.A.B. Abdullah, F.K. Loong, T.S. Jin, N.H. Teng, M. Nabiałek, B. Jeż, N.Y. Sing, Evaluation of the effect of silica fume on amorphous fly ash geopolymers exposed to elevated temperature, Magnetochemistry. 7 (2021) 1–14, https://doi.org/10.3390/magnetochemistry7010009.

[18] M.E. Kalaw, J.M. Adiarte, R.D. Cruz, K.M. Martinez, C.A. Vega, M.A. Promentilla, Strength and fire resistance characteristics of geopolymers synthesized from volcanic ash, red clay and waste pen shells, IOP Conf. Ser.: Mater. Sci. Eng. 1109 (1) (2021) 012068, https://doi.org/10.1088/1757-899X/1109/1/012068.

[19] M. Lahoti, K.K. Wong, K.H. Tan, E.-H. Yang, Effect of alkali cation type on strength endurance of fly ash geopolymers subject to high temperature exposure, Mater. Des. 154 (2018) 8–19.

[20] D. Yan, Y. Zhang, S. Chen, H. Fazli, Y. Liu, Y. Ao, Effect of silica moduli on the thermal degradation mechanisms of fly ash-based geopolymer mortars, J. Mater. Civ. Eng. 33 (2021) 4021059.

[21] Y. Luna-Galiano, C. Fernández-Pereira, M. Izquierdo, Contributions to the study of porosity in fly ash-based geopolymers. Relationship between degree of reaction, porosity and compressive strength, Mater. Construcción. 66 (324) (2016) e098–e098.

[22] W.D.A. Rickard, J. Temuujin, A. van Riessen, Thermal analysis of geopolymer pastes synthesised from five fly ashes of variable composition, J. Non. Cryst. Solids. 358 (15) (2012) 1830–1839, https://doi.org/10.1016/j.jnoncrysol.2012.05.032.

[23] L. Vickers, W.D.A. Rickard, A. Van Riessen, Strategies to control the high temperature shrinkage of fly ash based geopolymers, Thermochim. Acta. 580 (2014) 20–27, https://doi.org/10.1016/j.tca.2014.01.020.

[24] M. Lahoti, K.H. Tan, E.-H. Yang, A critical review of geopolymer properties for structural fire-resistance applications, Constr. Build. Mater. 221 (2019) 514–526, https://doi.org/10.1016/j.conbuildmat.2019.06.076.

[25] W.D.A. Rickard, R. Williams, J. Temuujin, A. van Riessen, Assessing the suitability of three Australian fly ashes as an aluminosilicate source for geopolymers in high temperature applications, Mater. Sci. Eng. A. 528 (9) (2011) 3390–3397, https://doi.org/10.1016/j.msea.2011.01.005.

[26] R.T. Hemmings, E.E. Berry, On the glass in coal fly ashes: recent advances, MRS Proc. 113 (1987).

[27] D.M. Roy, K. Luke, S. Diamond, Characterization of fly ash and its reactions in concrete, in: Mater. Res. Soc. Symp. Proc., 1985, https://doi.org/10.1557/proc-43-3.

[28] A. Bhatt, S. Priyadarshini, A.A. Mohanakrishnan, A. Abri, M. Sattler, S. Techapaphawit, Physical, chemical, and geotechnical properties of coal fly ash: a global review, Case Stud. Constr. Mater. 11 (2019), e00263.

[29] A. Fernández-Jiménez, A. Palomo, Characterisation of fly ashes. Potential reactivity as alkaline cements, Fuel 82 (18) (2003) 2259–2265, https://doi.org/10.1016/S0016-2361(03)00194-7.

[30] F.U.A. Shaikh, 23 - Fibre-reinforced geopolymer composites (FRGCs) for structural applications, in: I.M.B.T.-A. in C.M.C. (Second E. Low (Ed.), Woodhead Publ. Ser. Compos. Sci. Eng., Woodhead Publishing, 2014: pp. 569–593. doi:10.1016/B978-0-08-102166-8.00023-2.

[31] D. Glosser, A. Choudhary, O.B. Isgor, W.J. Weiss, Investigation of reactivity of fly ash and its effect on mixture properties, ACI Mater. J. 116 (2019) 193–200.

[32] H.S. Pietersen, A.L.A. Fraay, J.M. Bijen, Reactivity of fly ash at high pH, MRS Online Proc. Libr. Arch. 178 (1989), https://doi.org/10.1557/PROC-178-139.

[33] A. Fernandezjimenez, A. Delatorre, A. Palomo, G. Lopezolmo, M. Alonso, M. Aranda, Quantitative determination of phases in the alkali activation of fly ash. Part I. Potential ash reactivity, Fuel. 85 (5-6) (2006) 625–634.

[34] K.U. Ambikakumari Sanalkumar, M. Lahoti, E.-H. Yang, Investigating the potential reactivity of fly ash for geopolymerization, Constr. Build. Mater. 225 (2019) 283–291. doi:10.1016/j.conbuildmat.2019.07.140.

[35] J.L. Provis, J.S.J. Van Deventer, Geopolymers: Structures, processing, properties and industrial applications, Elsevier Ltd (2009), https://doi.org/10.1533/9781845696382.

[36] J.L. Provis, C.Z. Yong, P. Duxson, J.S.J. van Deventer, Correlating mechanical and thermal properties of sodium silicate-fly ash geopolymers, Colloids Surf. A Physicochem. Eng. Asp. 336 (1-3) (2009) 57–63, https://doi.org/10.1016/j.colsurfa.2008.11.019.

[37] L.P. Singh, S.R. Karade, S.K. Bhattacharyya, M.M. Yousuf, S. Ahalawat, Beneficial role of nanosilica in cement based materials–a review, Constr. Build. Mater. 47 (2013) 1069–1077.

[38] E.D. Rodríguez, S.A. Bernal, J.L. Provis, J. Paya, J.M. Monzo, M.V. Borrachero, Effect of nanosilica-based activators on the performance of an alkali-activated fly ash binder, Cem. Concr. Compos. 35 (1) (2013) 1–11.

[39] S.K. Saxena, M. Kumar, N.B. Singh, Fire Resistant Properties of Alumino Silicate Geopolymer cement Mortars, Mater. Today Proc. 4 (4) (2017) 5605–5612, https://doi.org/10.1016/j.matpr.2017.06.018.

[40] F. Shaikh, S. Haque, Effect of nano silica and fine silica sand on compressive strength of sodium and potassium activators synthesised fly ash geopolymer at elevated temperatures, Fire Mater. 42 (3) (2018) 324–335, https://doi.org/10.1002/fam.2496.

[41] S. Wattanasiriwech, F.A. Nurgesang, D. Wattanasiriwech, P. Timakul, Characterisation and properties of geopolymer composites. Part 2: Role of cordierite-mullite reinforcement, Ceram. Int. 43 (18) (2017) 16063–16069, https://doi.org/10.1016/j.ceramint.2017.08.215.

[42] M.N.N. Khan, P.K. Sarker, Effect of waste glass fine aggregate on the strength, durability and high temperature resistance of alkali-activated fly ash and GGBFS blended mortar, Constr. Build. Mater. 263 (2020), 120177.

[43] X. Jiang, R. Xiao, Y. Ma, M. Zhang, Y. Bai, B. Huang, Influence of waste glass powder on the physico-mechanical properties and microstructures of fly ash-based geopolymer paste after exposure to high temperatures, Constr. Build. Mater. 262 (2020), 120579.

[44] S.A. Bernal, J. Bejarano, C. Garzón, R. Mejía de Gutiérrez, S. Delvasto, E. D. Rodríguez, Performance of refractory aluminosilicate particle / fiber-reinforced geopolymer composites, Compos. Part B 43 (4) (2012) 1919–1928.

[45] L. Carabba, R. Moricone, G.E. Scarponi, A. Tugnoli, M.C. Bignozzi, Alkali activated lightweight mortars for passive fire protection: a preliminary study, Constr. Build. Mater. 195 (2019) 75–84, https://doi.org/10.1016/j.conbuildmat.2018.11.005.

[46] I. Ozer, S. Soyer-Uzun, Relations between the structural characteristics and compressive strength in metakaolin based geopolymers with different molar Si/Al ratios, Ceram. Int. 41 (8) (2015) 10192–10198, https://doi.org/10.1016/j.ceramint.2015.04.125.

[47] P. Duxson, S.W. Mallicoat, G.C. Lukey, W.M. Kriven, J.S.J. van Deventer, The effect of alkali and Si/Al ratio on the development of mechanical properties of metakaolin-based geopolymers, Colloids Surf. A Physicochem. Eng. Asp. 292 (1) (2007) 8–20, https://doi.org/10.1016/j.colsurfa.2006.05.044.

[48] P.V. Krivenko, G.Y. Kovalchuk, Directed synthesis of alkaline aluminosilicate minerals in a geocement matrix, J. Mater. Sci. 42 (9) (2007) 2944–2952, https://doi.org/10.1007/s10853-006-0528-3.

[49] D.L.Y. Kong, J.G. Sanjayan, Effect of elevated temperatures on geopolymer paste, mortar and concrete, Cem. Concr. Res. 40 (2) (2010) 334–339.

[50] K. Dombrowski, A. Buchwald, M. Weil, The influence of calcium content on the structure and thermal performance of fly ash based geopolymers, J. Mater. Sci. 42 (9) (2007) 3033–3043, https://doi.org/10.1007/s10853-006-0532-7.

[51] P.K. Sarker, S. Kelly, Z. Yao, Effect of fire exposure on cracking, spalling and residual strength of fly ash geopolymer concrete, Mater. Des. 63 (2014) 584–592, https://doi.org/10.1016/j.matdes.2014.06.059.

[52] A. Nazari, A. Bagheri, J.G. Sanjayan, M. Dao, C. Mallawa, P. Zannis, S. Zumbo, Thermal shock reactions of Ordinary Portland cement and geopolymer concrete: Microstructural and mechanical investigation, Constr. Build. Mater. 196 (2019) 492–498, https://doi.org/10.1016/j.conbuildmat.2018.11.098.

[53] N. Ranjbar, M. Mehrali, U.J. Alengaram, H.S.C. Metselaar, M.Z. Jumaat, Compressive strength and microstructural analysis of fly ash/palm oil fuel ash based geopolymer mortar under elevated temperatures, Constr. Build. Mater. 65 (2014) 114–121, https://doi.org/10.1016/j.conbuildmat.2014.04.064.

[54] W.D.A. Rickard, C.S. Kealley, A. van Riessen, J. Biernaki, Thermally induced microstructural changes in fly ash geopolymers: experimental results and proposed model, J. Am. Ceram. Soc. 98 (3) (2015) 929–939.

[55] F.U.A. Shaikh, V. Vimonsatit, Compressive strength of fly-ash-based geopolymer concrete at elevated temperatures, Fire Mater. 39 (2) (2015) 174–188, https://doi.org/10.1002/fam.2240.

[56] S. Wattanasiriwech, F.A. Nurgesang, D. Wattanasiriwech, P. Timakul, Characterisation and properties of geopolymer composite part 1: Role of mullite reinforcement, Ceram. Int. 43 (2017) 16055–16062.

[57] H. Zhang, L. Li, C. Yuan, Q. Wang, P.K. Sarker, X. Shi, Deterioration of ambient-cured and heat-cured fly ash geopolymer concrete by high temperature exposure and prediction of its residual compressive strength, Constr. Build. Mater. 262 (2020), 120924.

[58] T.W. Cheng, J.P. Chiu, Fire-resistant geopolymer produce by granulated blast furnace slag, Miner. Eng. 16 (2003) 205–210, https://doi.org/10.1016/S0892-6875(03)00008-6.

[59] J. Cai, X. Li, J. Tan, B. Vandevyvere, Thermal and compressive behaviors of fly ash and metakaolin-based geopolymer, J. Build. Eng. 30 (2020), 101307, https://doi.org/10.1016/j.jobe.2020.101307.

[60] Sindhunata, J.S.J. van Deventer, G.C. Lukey, H. Xu, Xu, Effect of curing temperature and silicate concentration on fly-ash-based geopolymerization, Ind. Eng. Chem. Res. 45 (10) (2006) 3559–3568, https://doi.org/10.1021/ie051251p.

[61] F. Uddin Ahmed Shaikh, S. Haque, J. Sanjayan, Behavior of fly ash geopolymer as fire resistant coating for timber, J. Sustain. Cem. Mater. 8 (5) (2019) 259–274, https://doi.org/10.1080/21650373.2018.1537015.

[62] Z. Pan, J.G. Sanjayan, Factors influencing softening temperature and hot-strength of geopolymers, Cem. Concr. Compos. 34 (2) (2012) 261–264, https://doi.org/10.1016/j.cemconcomp.2011.09.019.

[63] H.Y. Zhang, V. Kodur, B. Wu, J. Yan, Z.S. Yuan, Effect of temperature on bond characteristics of geopolymer concrete, Constr. Build. Mater. 163 (2018) 277–285, https://doi.org/10.1016/j.conbuildmat.2017.12.043.

[64] S. Luhar, S. Chaudhary, I. Luhar, Thermal resistance of fly ash based rubberized geopolymer concrete, J. Build. Eng. 19 (2018) 420–428, https://doi.org/10.1016/j.jobe.2018.05.025.

[65] D.L.Y. Kong, J.G. Sanjayan, K. Sagoe-Crentsil, Comparative performance of geopolymers made with metakaolin and fly ash after exposure to elevated temperatures, Cem. Concr. Res. 37 (12) (2007) 1583–1589, https://doi.org/10.1016/j.cemconres.2007.08.021.

[66] Z. Pan, J.G. Sanjayan, B.V. Rangan, An investigation of the mechanisms for strength gain or loss of geopolymer mortar after exposure to elevated temperature, J. Mater. Sci. 44 (7) (2009) 1873–1880, https://doi.org/10.1007/s10853-009-3243-z.

[67] D.L.Y. Kong, J.G. Sanjayan, Damage behavior of geopolymer composites exposed to elevated temperatures, Cem. Concr. Compos. 30 (10) (2008) 986–991, https://doi.org/10.1016/j.cemconcomp.2008.08.001.

[68] A. Hosan, S. Haque, F. Shaikh, Compressive behaviour of sodium and potassium activators synthetized fly ash geopolymer at elevated temperatures: a comparative study, J. Build. Eng. 8 (2016) 123–130, https://doi.org/10.1016/j.jobe.2016.10.005.

[69] S.M. Park, J.G. Jang, N.K. Lee, H.K. Lee, Physicochemical properties of binder gel in alkali-activated fly ash/slag exposed to high temperatures, Cem. Concr. Res. 89 (2016) 72–79, https://doi.org/10.1016/j.cemconres.2016.08.004.

[70] P.W.J.G. Wijnen, T.P.M. Beelen, J.W. De Haan, L.J.M. Van De Ven, R.A. Van Santen, The structure directing effect of cations in aqueous silicate solutions. A 29Si-NMR study, Colloids Surf. 45 (1990) 255–268, https://doi.org/10.1016/0166-6622(90)80029-4.

[71] P. Duxson, G.C. Lukey, F. Separovic, J.S.J. van Deventer, Effect of alkali cations on aluminum incorporation in geopolymeric gels, Ind. Eng. Chem. Res. 44 (4) (2005) 832–839, https://doi.org/10.1021/ie0494216.

[72] A. Fernández-Jiménez, A. Palomo, M. Criado, Alkali activated fly ash binders. A comparative study between sodium and potassium activators [Activación alcalina de cenizas volantes. Estudio comparativo entre activadores sódicos y potásicos], Mater. Construcción. 56 (2006) 51–65, https://doi.org/10.3989/mc.2006.v56.i281.92.

[73] M. Carrillo-Tripp, H. Saint-Martin, I. Ortega-Blake, A comparative study of the hydration of Na+ and K+ with refined polarizable model potentials, J. Chem. Phys. 118 (15) (2003) 7062–7073, https://doi.org/10.1063/1.1559673.

[74] I. Barin, Thermochemical Data of Pure Substances, 1995. doi:10.1002/9783527619825.

[75] T. Doan, P. Louda, D. Kroisova, O. Bortnovsky, N. Thang, New generation of geopolymer composite for fire-resistance, Adv. Compos. Mater. - Anal. Nat. Man-Made Mater. (2011), https://doi.org/10.5772/17933.

[76] T. Bakharev, Thermal behaviour of geopolymers prepared using class F fly ash and elevated temperature curing, Cem. Concr. Res. 36 (6) (2006) 1134–1147, https://doi.org/10.1016/j.cemconres.2006.03.022.

[77] H. Van Vlack, Physical Ceramics for Engineers, Addison, Wesley, London, 1964, pp. 94–102.

[78] M. Taylor, G.E. Brown, Structure of mineral glasses-I. The feldspar glasses NaAlSi3O8, KAlSi3O8, CaAl2Si2O8, Geochim. Cosmochim. Acta. 43 (1) (1979) 61–75, https://doi.org/10.1016/0016-7037(79)90047-4.

[79] V.F.F. Barbosa, K.J.D. MacKenzie, Synthesis and thermal behaviour of potassium sialate geopolymers, Mater. Lett. 57 (9-10) (2003) 1477–1482, https://doi.org/10.1016/S0167-577X(02)01009-1.

[80] M. Lizcano, A. Gonzalez, S. Basu, K. Lozano, M. Radovic, D. Viehland, Effects of water content and chemical composition on structural properties of alkaline activated metakaolin-based geopolymers, J. Am. Ceram. Soc. 95 (7) (2012) 2169–2177, https://doi.org/10.1111/j.1551-2916.2012.05184.x.

[81] M. Lizcano, H.S. Kim, S. Basu, M. Radovic, Mechanical properties of sodium and potassium activated metakaolin-based geopolymers, J. Mater. Sci. 47 (6) (2012) 2607–2616, https://doi.org/10.1007/s10853-011-6085-4.

[82] P. Duxson, J.L. Provis, G.C. Lukey, S.W. Mallicoat, W.M. Kriven, J.S.J. van Deventer, Understanding the relationship between geopolymer composition, microstructure and mechanical properties, Colloids Surf. A Physicochem. Eng. Asp. 269 (1-3) (2005) 47–58, https://doi.org/10.1016/j.colsurfa.2005.06.060.

[83] H. Xu, J.S.J. van Deventer, The effect of alkali metals on the formation of geopolymeric gels from alkali-feldspars, Colloids Surf. A Physicochem. Eng. Asp. 216 (1-3) (2003) 27–44, https://doi.org/10.1016/S0927-7757(02)00499-5.

[84] K. Okada, A. Ooyama, T. Isobe, Y. Kameshima, A. Nakajima, K.J.D. MacKenzie, Water retention properties of porous geopolymers for use in cooling applications, J. Eur. Ceram. Soc. 29 (10) (2009) 1917–1923, https://doi.org/10.1016/j.jeurceramsoc.2008.11.006.

[85] L. Vitola, I. Pundiene, J. Pranckeviciene, D. Bajare, The Impact of the Amount of Water Used in Activation Solution and the Initial Temperature of Paste on the Rheological Behaviour and Structural Evolution of Metakaolin-Based Geopolymer Pastes, Sustainability. 12 (2020) 8216.

[86] Z. Zuhua, Y. Xiao, Z. Huajun, C. Yue, Role of water in the synthesis of calcined kaolin-based geopolymer, Appl. Clay Sci. 43 (2) (2009) 218–223, https://doi.org/10.1016/j.clay.2008.09.003.

[87] V.F.F. Barbosa, K.J.D. Mackenzie, Thermal behaviour of inorganic geopolymers and composites derived from sodium polysialate, 38 (2003) 319–331.

[88] I. Barin, Thermochemical data of pure substances, Wiley (1995), https://doi.org/10.1002/9783527619825.

[89] J.C. Swanepoel, C.a. Strydom, Utilisation of fly ash in a geopolymeric material, Appl. Geochem. 17 (2002) 1143–1148, https://doi.org/10.1016/S0883-2927(02)00005-7.

[90] S. Kumar, R. Kumar, Mechanical activation of fly ash: effect on reaction, structure and properties of resulting geopolymer, Ceram. Int. 37 (2011) 533–541, https://doi.org/10.1016/j.ceramint.2010.09.038.

[91] M.M.A.B. Abdullah, H. Kamarudin, M. Bnhussain, I. Khairul Nizar, A.R. Rafiza, Y. Zarina, The relationship of NaOH molarity, Na2SiO3/NaOH ratio, fly ash/alkaline activator ratio, and curing temperature to the strength of fly ash-based geopolymer, in: Adv. Mater. Res., Trans Tech Publ, 2011: pp. 1475–1482.

[92] G.S. Ryu, Y.B. Lee, K.T. Koh, Y.S. Chung, The mechanical properties of fly ash-based geopolymer concrete with alkaline activators, Constr. Build. Mater. 47 (2013) 409–418, https://doi.org/10.1016/j.conbuildmat.2013.05.069.

[93] D. Hardjito, B.V. Rangan, Development and properties of low-calcium fly ash-based geopolymer concrete, Perth, 2005. http://www.geopolymer.org/fichiers_pdf/curtin-flyash-GP-concrete-report.pdf (accessed June 13, 2012).

[94] F. Canpolat, T.R. Naik, Effect of curing conditions on strength and durability of high-performance concrete, Sci. Iran. 24 (2017) 576–583, https://doi.org/10.24200/sci.2017.2419.

[95] R.T. Chancey, P. Stutzman, M.C.G. Juenger, D.W. Fowler, Comprehensive phase characterization of crystalline and amorphous phases of a Class F fly ash, Cem. Concr. Res. 40 (1) (2010) 146–156, https://doi.org/10.1016/j.cemconres.2009.08.029.

[96] P. Nath, P.K. Sarker, Effect of GGBFS on setting, workability and early strength properties of fly ash geopolymer concrete cured in ambient condition, Constr. Build. Mater. 66 (2014) 163–171, https://doi.org/10.1016/j.conbuildmat.2014.05.080.

[97] P.S. Deb, P. Nath, P.K. Sarker, The effects of ground granulated blast-furnace slag blending with fly ash and activator content on the workability and strength properties of geopolymer concrete cured at ambient temperature, Mater. Des. 62 (2014) 32–39, https://doi.org/10.1016/j.matdes.2014.05.001.

[98] B. Udvardi, K. Róman, E. Kurovics, R. Géber, I. Kocserha, Preparation and investigation of geopolymers generated from construction, demolition and industrial wastes, WIT Trans. Eng. Sci. 124 (2019) 49–59.

[99] A.M. Kaja, A. Lazaro, Q.L. Yu, Effects of Portland cement on activation mechanism of class F fly ash geopolymer cured under ambient conditions, Constr. Build. Mater. 189 (2018) 1113–1123, https://doi.org/10.1016/j.conbuildmat.2018.09.065.

[100] E. Tajuelo Rodriguez, K. Garbev, D. Merz, L. Black, I.G. Richardson, Thermal stability of C-S-H phases and applicability of Richardson and Groves' and Richardson C-(A)-S-H(I) models to synthetic C-S-H, Cem. Concr. Res. 93 (2017) 45–56, https://doi.org/10.1016/j.cemconres.2016.12.005.

[101] W.K.W. Lee, J.S.J. van Deventer, The effect of ionic contaminants on the early-age properties of alkali-activated fly ash-based cements, Cem. Concr. Res. 32 (4) (2002) 577–584, https://doi.org/10.1016/S0008-8846(01)00724-4.

[102] J. Temuujin, A. van Riessen, R. Williams, Influence of calcium compounds on the mechanical properties of fly ash geopolymer pastes, J. Hazard. Mater. 167 (1-3) (2009) 82–88, https://doi.org/10.1016/j.jhazmat.2008.12.121.

[103] R. Świetlik, M. Trojanowska, M.A. Jóźwiak, Evaluation of the distribution of heavy metals and their chemical forms in ESP-fractions of fly ash, Fuel Process. Technol. 95 (2012) 109–118.

[104] T.A. Vereshchagina, N.N. Anshits, N.G. Maksimov, S.N. Vereshchagin, O. A. Bayukov, A.G. Anshits, The nature and properties of iron-containing nanoparticles dispersed in an aluminosilicate matrix of cenospheres, Glas. Phys. Chem. 30 (3) (2004) 247–256.

[105] W.D.A. Rickard, A. Van Riessen, P. Walls, Thermal character of geopolymers synthesized from class F Fly ash containing high concentrations of iron and α-quartz, Int. J. Appl. Ceram. Technol. 7 (2010) 81–88, https://doi.org/10.1111/j.1744-7402.2008.02328.x.

[106] R. Williams, Characterisation of Fly Ash for production of Geopolymer, Honours Diss. Curtin Univ. Technol. Perth, Aust. (2006).

[107] K.M. Klima, K. Schollbach, H.J.H. Brouwers, Q. Yu, Enhancing the thermal performance of Class F fly ash-based geopolymer by sodalite (2021) (Manuscript accepted by CBM, in press), (n.d.) 1–34.

[108] M.W. McElhinny, P.L.B.T.-I.G. McFadden, eds., Chapter Two - Rock Magnetism, in: Paleomagnetism, Academic Press, 2000: pp. 31–77. doi:10.1016/S0074-6142(00)80095-9.

[109] T. Yang, Q. Wu, H. Zhu, Z. Zhang, Geopolymer with improved thermal stability by incorporating high-magnesium nickel slag, Constr. Build. Mater. 155 (2017) 475–484, https://doi.org/10.1016/j.conbuildmat.2017.08.081.

[110] F. Jin, K. Gu, A. Al-Tabbaa, Strength and hydration properties of reactive MgO-activated ground granulated blastfurnace slag paste, Cem. Concr. Compos. 57 (2015) 8–16, https://doi.org/10.1016/j.cemconcomp.2014.10.007.

[111] A.M. Rashad, S.R. Zeedan, The effect of activator concentration on the residual strength of alkali-activated fly ash pastes subjected to thermal load, Constr. Build. Mater. 25 (7) (2011) 3098–3107, https://doi.org/10.1016/j.conbuildmat.2010.12.044.

[112] I. Ismail, S.A. Bernal, J.L. Provis, R. San Nicolas, S. Hamdan, J.S.J. van Deventer, Modification of phase evolution in alkali-activated blast furnace slag by the incorporation of fly ash, Cem. Concr. Compos. 45 (2014) 125–135, https://doi.org/10.1016/j.cemconcomp.2013.09.006.

[113] T. Bakharev, Durability of geopolymer materials in sodium and magnesium sulfate solutions, Cem. Concr. Res. 35 (6) (2005) 1233–1246, https://doi.org/10.1016/j.cemconres.2004.09.002.

[114] A. Fernández-Jiménez, N. Cristelo, T. Miranda, Á. Palomo, Sustainable alkali activated materials: precursor and activator derived from industrial wastes, J. Clean. Prod. 162 (2017) 1200–1209, https://doi.org/10.1016/j.jclepro.2017.06.151.

[115] P. Rożek, M. Król, W. Mozgawa, Geopolymer-zeolite composites: a review, J. Clean. Prod. 230 (2019) 557–579, https://doi.org/10.1016/j.jclepro.2019.05.152.

[116] M.-X. Xu, Y. He, Y.-P. Wang, X.-M. Cui, Preparation of a non-hydrothermal NaA zeolite membrane and defect elimination by vacuum-inhalation repair method, Chem. Eng. Sci. 158 (2017) 117–123, https://doi.org/10.1016/j.ces.2016.10.001.

[117] E. Álvarez-Ayuso, X. Querol, F. Plana, A. Alastuey, N. Moreno, M. Izquierdo, O. Font, T. Moreno, S. Diez, E. Vázquez, M. Barra, Environmental, physical and structural characterisation of geopolymer matrixes synthesised from coal (co-) combustion fly ashes, J. Hazard. Mater. 154 (1-3) (2008) 175–183, https://doi.org/10.1016/j.jhazmat.2007.10.008.

[118] W.M.K. Manuel E. Brito, Eldon Case, Developments in Porous, Biological and Geopolymer Ceramics, 2007. doi:10.1002/9780470339749.

[119] B. Jha, D.N. Singh, Fly Ash Zeolites: Innovations, applications and directions, 2016. doi:10.1007/978-981-10-1404-8.

[120] C. Kosanovic, B. Subotic, I. Smit, Thermally induced phase transformations in cation-exchanged zeolites 4A, 13X and synthetic mordenite and their amorphous derivatives obtained by mechanochemical treatment, Thermochim. Acta. 317 (1) (1998) 25–37, https://doi.org/10.1016/S0040-6031(98)00353-0.

[121] T. Carey, Chemical Control of Thermal Expansion in Zeolites with the LTA Topology, (2013). http://etheses.bham.ac.uk/4258/1/Carey13PhD.pdf.

[122] T. Kihara, A. Mikuni, Y. Nakamura, R. Komatsu, K. Ikeda, Consolidation of Pressurised Fluidised Bed Combustion Ash (PF-Ash) by the geopolymer technique at ambient temperature, Adv. Sci. Technol. 34 (2002) 163–168.

[123] H. Takeda, S. Hashimoto, H. Yokoyama, S. Honda, Y. Iwamoto, Characterization of zeolite in zeolite-geopolymer hybrid bulk materials derived from kaolinitic clays, Materials (Basel). 6 (2013) 1767–1778, https://doi.org/10.3390/ma6051767.

[124] P. Sturm, G.J.G. Gluth, S. Simon, H.J.H. Brouwers, H.-C. Kühne, The effect of heat treatment on the mechanical and structural properties of one-part geopolymer-zeolite composites, Thermochim. Acta. 635 (2016) 41–58, https://doi.org/10.1016/j.tca.2016.04.015.

[125] L.P. van Reeuwijk, The thermal dehydration of natural zeolites, (1974).

[126] Z. Pan, J.G. Sanjayan, Stress-strain behaviour and abrupt loss of stiffness of geopolymer at elevated temperatures, Cem. Concr. Compos. 32 (9) (2010) 657–664, https://doi.org/10.1016/j.cemconcomp.2010.07.010.

[127] D. Kong, J. Sanjayan, K. Sagoe-Crentsil, The behaviour of geopolymer paste and concrete at elevated temperatures, Int. Conf. Pozzolan, Concr. Geopolymer, Khon Kaen Univ. Khon Kaen, Thail. (2006), Pp. 105-119. (2006).

[128] K.M. Klima, K. Schollbach, H.J.H. Brouwers, Q. Yu, Enhancing the thermal performance of Class F fly ash-based geopolymer by sodalite, Constr. Build. Mater. 314 (2022), 125574.

[129] Z. Pan, J.G. Sanjayan, F. Collins, Effect of transient creep on compressive strength of geopolymer concrete for elevated temperature exposure, Cem. Concr. Res. 56 (2014) 182–189, https://doi.org/10.1016/j.cemconres.2013.11.014.

[130] P. Duxson, G.C. Lukey, J.S.J. Van Deventer, Physical evolution of Na-geopolymer derived from metakaolin up to 1000 °c, J. Mater. Sci. 42 (2007) 3044–3054, https://doi.org/10.1007/s10853-006-0535-4.

[131] P. Ptáček, F. Soukal, T. Opravil, E. Bartoníčková, J. Wasserbauer, The formation of feldspar strontian (SrAl2Si2O8) via ceramic route: Reaction mechanism, kinetics and thermodynamics of the process, Ceram. Int. 42 (2016) 8170–8178.

[132] J.M. Branlund, A.M. Hofmeister, Heat transfer in plagioclase feldspars, Am. Mineral. 97 (7) (2012) 1145–1154.

[133] J.H. Perry, Chemical engineers' handbook, J. Chem. Educ. 27 (9) (1950) 533, https://doi.org/10.1021/ed027p533.1.

[134] S. Alehyen, M. Zerzouri, M. El Alouani, M. El Achouri, M. Taibi, Porosity and fire resistance of fly ash based geopolymer, J. Mater. Environ. Sci. 8 (2017) 3676–3689.

[135] R. Kumar, S.S. Mayengbam, Enhancement of the thermal durability of fly ash-based geopolymer paste by incorporating potassium feldspar, J. Inst. Eng. Ser. A. 102 (1) (2021) 175–183.

[136] R.N. Thakur, S. Ghosh, Effect of mix composition on compressive strength and microstructure of fly ash based geopolymer composites, J. Eng. Appl. Sci. 4 (2009) 68–74, https://doi.org/10.1016/j.actamat.2006.08.032.

[137] Z. Zhang, J.L. Provis, A. Reid, H. Wang, Mechanical, thermal insulation, thermal resistance and acoustic absorption properties of geopolymer foam concrete, Cem. Concr. Compos. 62 (2015) 97–105, https://doi.org/10.1016/j.cemconcomp.2015.03.013.

[138] M.W. Hussin, M.A.R. Bhutta, M. Azreen, P.J. Ramadhansyah, J. Mirza, Performance of blended ash geopolymer concrete at elevated temperatures, Mater. Struct. Constr. 48 (3) (2015) 709–720, https://doi.org/10.1617/s11527-014-0251-5.

[139] C.W. Bale, E. Bélisle, P. Chartrand, S.A. Decterov, G. Eriksson, A.E. Gheribi, K. Hack, I.-H. Jung, Y.-B. Kang, J. Melançon, A.D. Pelton, S. Petersen, C. Robelin, J. Sangster, P. Spencer, M.-A. Van Ende, FactSage thermochemical software and databases, 2010–2016, Calphad Comput. Coupling Phase Diagrams Thermochem. 54 (2016) 35–53, https://doi.org/10.1016/j.calphad.2016.05.002.

[140] S. Wang, C. Zhang, J. Chen, Utilization of Coal Fly Ash for the Production of Glass-ceramics With Unique Performances: A Brief Review, J. Mater. Sci. Technol. 30 (12) (2014) 1208–1212, https://doi.org/10.1016/j.jmst.2014.10.005.

[141] J.L. Provis, P. Duxson, G.C. Lukey, J.S.J. van Deventer, Statistical thermodynamic model for Si/Al ordering in amorphous aluminosilicates, Chem. Mater. 17 (11) (2005) 2976–2986.

[142] V.D. Cao, S. Pilehvar, C. Salas-Bringas, A.M. Szczotok, J.F. Rodriguez, M. Carmona, N. Al-Manasir, A.-L. Kjøniksen, Microencapsulated phase change materials for enhancing the thermal performance of Portland cement concrete and geopolymer concrete for passive building applications, Energy Convers. Manag. 133 (2017) 56–66.

[143] A. Hassan, M. Arif, M. Shariq, Influence of microstructure of geopolymer concrete on its mechanical properties—a review, Adv. Sustain. Constr. Mater. Geotech. Eng. (2020) 119–129.

[144] M.Z.N. Khan, F.U.A. Shaikh, Y. Hao, H. Hao, Synthesis of high strength ambient cured geopolymer composite by using low calcium fly ash, Constr. Build. Mater. 125 (2016) 809–820.

[145] A.Z.M. Ali, J. Sanjayan, The spalling of geopolymer high strength concrete wall panels and cylinders under hydrocarbon fire, in: MATEC Web Conf., EDP Sciences, 2016: p. 2005.

[146] P.K. Sarker, S. McBeath, Fire endurance of steel reinforced fly ash geopolymer concrete elements, Constr. Build. Mater. 90 (2015) 91–98, https://doi.org/10.1016/j.conbuildmat.2015.04.054.

[147] F. Colangelo, R. Cioffi, G. Roviello, I. Capasso, D. Caputo, P. Aprea, B. Liguori, C. Ferone, Thermal cycling stability of fly ash based geopolymer mortars, Compos. Part b Eng. 129 (2017) 11–17.

[148] H.Y. Zhang, G.H. Qiu, V. Kodur, Z.S. Yuan, Spalling behavior of metakaolin-fly ash based geopolymer concrete under elevated temperature exposure, Cem. Concr. Compos. 106 (2020), 103483.

[149] Y. Luo, S.H. Li, K.M. Klima, H.J.H. Brouwers, Q. Yu, Degradation mechanism of hybrid fly ash/slag based geopolymers exposed to elevated temperatures, Cem. Concr. Res. 151 (2022) 106649, https://doi.org/10.1016/j.cemconres.2021.106649.

[150] J.L. Bell, P.E. Driemeyer, W.M. Kriven, Formation of Ceramics from Metakaolin-Based Geopolymers. Part II: K-Based Geopolymer, J. Am. Ceram. Soc. 92 (2009) 607–615, https://doi.org/10.1111/j.1551-2916.2008.02922.x.

[151] D.D. Burduhos Nergis, M.M.A.B. Abdullah, A.V. Sandu, P. Vizureanu, XRD and TG-DTA Study of New Alkali Activated Materials Based on Fly Ash with Sand and Glass Powder, Materials (Basel) 13 (2020) 343, https://doi.org/10.3390/ma13020343.

[152] T. Kovářík, D. Rieger, J. Kadlec, T. Křenek, L. Kullová, M. Pola, P. Bělský, P. Franče, J. Říha, Thermomechanical properties of particle-reinforced geopolymer composite with various aggregate gradation of fine ceramic filler, Constr. Build. Mater. 143 (2017) 599–606, https://doi.org/10.1016/j.conbuildmat.2017.03.134.

[153] P. He, D. Jia, M. Wang, Y.u. Zhou, Thermal evolution and crystallization kinetics of potassium-based geopolymer, Ceram. Int. 37 (1) (2011) 59–63, https://doi.org/10.1016/j.ceramint.2010.08.008.

[154] F.N. Degirmenci, Freeze-Thaw and fire resistance of geopolymer mortar based on natural and waste pozzolans, Ceram. - Silikaty. 62 (2018) 41–49, https://doi.org/10.13168/cs.2017.0043.

[155] A.S. Rahman, D.W. Radford, Evaluation of the geopolymer/nanofiber interfacial bond strength and their effects on Mode-I fracture toughness of geopolymer matrix at high temperature, Compos. Interfaces. 24 (8) (2017) 817–831, https://doi.org/10.1080/09276440.2017.1279479.

[156] M. Sivasakthi, R. Jeyalakshmi, N.P. Rajamane, Investigation of Microstructure and Thermomechanical Properties of Nano-TiO2 Admixed Geopolymer for Thermal Resistance Applications, J. Mater. Eng. Perform. 30 (5) (2021) 3642–3653, https://doi.org/10.1007/s11665-021-05708-1.

[157] S.K. Shill, S. Al-Deen, M. Ashraf, W. Hutchison, Resistance of fly ash based geopolymer mortar to both chemicals and high thermal cycles simultaneously, Constr. Build. Mater. 239 (2020), 117886.

[158] E.A. Azimi, M.M.A.B. Abdullah, P. Vizureanu, M.A.A.M. Salleh, A.V. Sandu, J. Chaiprapa, S. Yoriya, K. Hussin, I.H. Aziz, Strength development and elemental

distribution of dolomite/fly ash geopolymer composite under elevated temperature, Materials (Basel). 13 (2020) 1015.

[159] X. Peng, Q. Shuai, H. Li, Q. Ding, Y. Gu, C. Cheng, Z. Xu, Fabrication and fireproofing performance of the coal fly ash-metakaolin-based geopolymer foams, Materials (Basel). 13 (2020) 1750.

[160] S. Yan, F. Zhang, X. Feng, J. Kong, B.o. Wang, J. Yang, Effect of high temperature on the mechanical properties of hierarchical porous cenosphere/geopolymer composite foams, Int. J. Appl. Ceram. Technol. 18 (3) (2021) 817–829.

[161] K. Dhasindrakrishna, K. Pasupathy, S. Ramakrishnan, J. Sanjayan, Progress, current thinking and challenges in geopolymer foam concrete technology, Cem. Concr. Compos. 116 (2021), 103886.

[162] R. Jacob, N. Trout, A. Solé, S. Clarke, A.I. Fernández, L.F. Cabeza, W. Saman, F. Bruno, Novel geopolymer for use as a sensible storage option in high temperature thermal energy storage systems, in: AIP Conf. Proc., AIP Publishing LLC, 2020: p. 190019.